# PREPARATION AND CHARACTERIZATION OF $RuO_2$ UNDER LAYER FOR PZT THIN FILMS

A Thesis Submitted

in Partial Fulfillment of the Requirements

for the Degree of

## MASTER OF TECHNOLOGY

*by*

PANKAJ MISRA

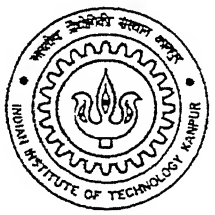


*to the*

MATERIALS SCIENCE PROGRAMME

INDIAN INSTITUTE OF TECHNOLOGY

KANPUR

Feb, 1998

# CERTIFICATE

It is certified that the work contained in the thesis entitled **Preparation and Characterization of $RuO_2$ under layer for PZT Thin Films** *by* **Mr. Pankaj Misra** has been carried out under our supervision and has not been submitted elsewhere for a degree.


Dr. Y.N. Mohapatra
Materials Sc. Programme.
and Dept. of Physics
Indian Instutute of Technology.
Kanpur.

Prof. D.C. Agrawal
Materials Science Programme.
Indian Instutute of Technology.
Kanpur

# DEDICATED TO

*my*

*LOVING PARENTS*

# Acknowledgement

I wish to express my deep sense of gratitude to my thesis supervisors prof. D. C. Agrawal and Dr. Y. N. Mohapatra for having given me a free rein in the formulation and implementation of the research work, and their expert guidence which helped me to be on the right track.

I am grateful to Dr. V.N. Kulkarni for allowing me to have free access to all the facilities for RBS measurements.

I wish to acknowledge my appreciations to my lab mate Subhashish for his useful suggestions and cooperation in sorting out many problems in my entire work. I wish to thank him for his encouraging words and brotherly advice which helped a lot in motivating me. I am indebted to friends like Atanu da, Tapo da and Giriji for their technical helps.

My special thanks are due to Pratyush for his help and cooperation throughout my programme. I would also like to thank Soumen, Indranil, Rasmi, Banashree, Atul, Mishraji and Ajit for making a lively working environment in the lab.

Last but not the least, I thank my family members for their constant source of encouragement throughout my academic programme.

# Abstract

$RuO_2$ thin films have been successfully deposited on Si substrates using solution chemistry technique. High resistivity n-type Si substrates were coated by spin coating method using 0.1M/litre $RuCl_3.nH_2O$ solution in ethanol. During the spin coating the spin speed was chosen as 4000 rpm and spinning time as 10 seconds. Repeated coating was performed to acheive desired thickness of $RuO_2$ film. After each coating the films were fired either at different temperatures (eg.,400, 450, 500, 550, 600, and 700°C) for fixed firing time (i.e. first layer for 10 minutes and subsequent layers for 2 minutes), or at fixed temperature (i.e. 500 and 550°C) for different times (eg. 2 to 10 minutes, with first layer fired for 10 minutes in each case). After detailed characterization of $RuO_2$/Si samples, PZT films were grown on it using sol-gel method, with 0.25 moles/litre precursor sol of PZT, at spin speed of 5000 rpm for 5 seconds. PZT samples grown on $RuO_2$ coated Si were fired at 400°C for 10 minutes and finally annealed at 700°C for 2 minutes either in air or in $O_2$ ambient.

Sheet resistance of $RuO_2$ film on Si was found to vary from 12.55 Ω /sq. to 20.30 Ω/sq. at various temperatures with minimum value of sheet resistance (7.25 and 7.79 Ω/sq.) being obtained in films fired at 500 and 550°C. Firing time i.e. 2 minutes or 5 minutes has no significant effect on sheet resistivity while firing at 10 minutes results in high value of sheet resistance. However at 500°C with 2 minutes firing , resistivity was found to be 1.41 μΩm. Sheet resistance was found to decrease linearly from 7.79 to 2.4 Ω/sq. with increasing number of coatings from 7 to 21. The change in sheet resistance is attributed to change in film thickness which was confirmed by RBS spectrometry. Some intermixing of constituents (Si, Ru) was also found above 500°C at $RuO_2$/Si interface.

PZT films grown on $RuO_2$ coated silicon exhibit perovskite phase in both cases (air and $O_2$ annealing). However, crystallization was much better in case of $O_2$ annealed films. PZT films begins to peel off beyond a thickness of 0.5 μ, perhaps due to stresses in the film. As films with thickness greater than 0.6 μ are needed for electrical characterization, the PZT films could not be charcterized with respect to their hysteresis loop and other electrical properties.

# Contents

# List of Figures

# List of Tables

# Chapter 1

# Introduction

Ferroelectricity, the reversal of spontaneous polarization by the applied electric field, was first discovered by Valasak in Rochelle salt (sodium potassium tartrate) in 1923. After this discovery, ferroelectrocity was reported in many more crystals like KDP (potassium dihydrogen phosphate), ADP (Ammonium dihydrogen phosphate)etc. But significant breakthrough in understanding the structural origin of ferroelectricity came through the discovery of the same in $BaTiO_3$ ceramic in 1945. The large dielectric and peizoelectric constant of these materials immediately made them attractive candidates for variety of applications. For many years ferroelectric dominated the field of sonar detector, phonographs pick ups and so on. Pyroelectric properties of these materials are utilized in fabrication of devices such as IR detectors etc. However none of these devices directly utilized the ferroelectric nature of the material namely large reversible spontaneous polarization. In the recent years this switchability of polarization has been demonstrated to have applications in nonvolatile memories for computer systems. Since then many laboratories all over the world are engaged in solving problems related to applications involving polarization reversal. In this thesis we investigate some aspects of ferroelectric capacitors directly relavent to such applications. Before starting our problem, we introduce the necessory concepts directly in the following section.

## 1.1 Ferroelectric Ceramics:

For the study of fundamental properties of the ferroelectric materials initially single crystal samples were used because they provide the advantage of having less imperfections and surface effects. Ferroelectric ceramic on the other hand have an advantage of being a great deal ea sier to prepare than their single crystal counterparts. In many

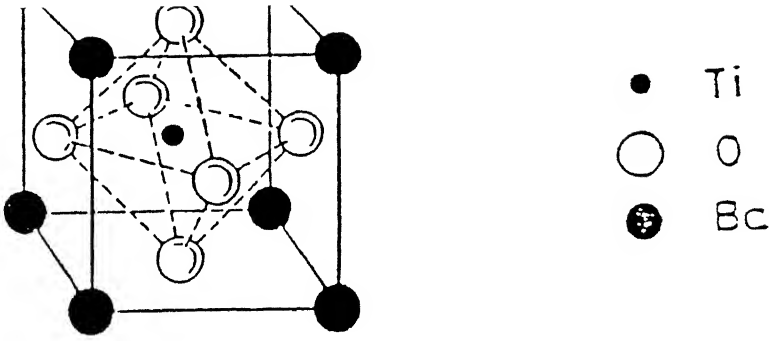


Figure 1.1: $ABO_3$ Structure(Ref.3)

cases they show ferroelectric properties approaching quite closely to those of single crystals. In addition it is possible to prepare wide range of ceramic composition, and to tailor the characteristics of the material properties for different applications.

Of the many known ferroelectric ceramics, lead based perovskite oxide solution such as lead titanate (PT), lead lanthanum titanate (PLT), lead zirconate titanate (PZT) are promising materials for research activities due to their superior pyroelectric, peizoelectric, optical, electrooptical and ferroelectric properties.

## 1.2 Lead Zirconate Titanate (PZT) Ceramics:

The lead zirconate titanate, a solid solution of lead oxide, zirconiate and titaniate chemically represented by $Pb(Zr_x\ Ti_(1-x))O_3$ is isostructural with the mineral Perovskite ($CaTiO_3$) and has $ABO_3$ type perovskite structure. The oxygen ions are at the face centered positions and the A and B sites are occupied by Pb ions and the Zr and Ti ions respectively Figure 1.1. The ceramic has cubic structure above certain temperature called Curie temperature and is paraelectric. On cooling below the Curie temperature , phase transition occurs to tetragonal, rhombohedral or orthorhombic structure depending upon Zr:Ti ratio. The phase diagram of PZT solid solution is shown in Figure 1.2. Now in the phase diagram of PZT solid solution a sharp phase boundary between the rhombohedral and the tetragonal phases called the MPB (Morphoteric phase boundary) exists at the composition 53% PZ. Enhanced peizoelectric coefficient,

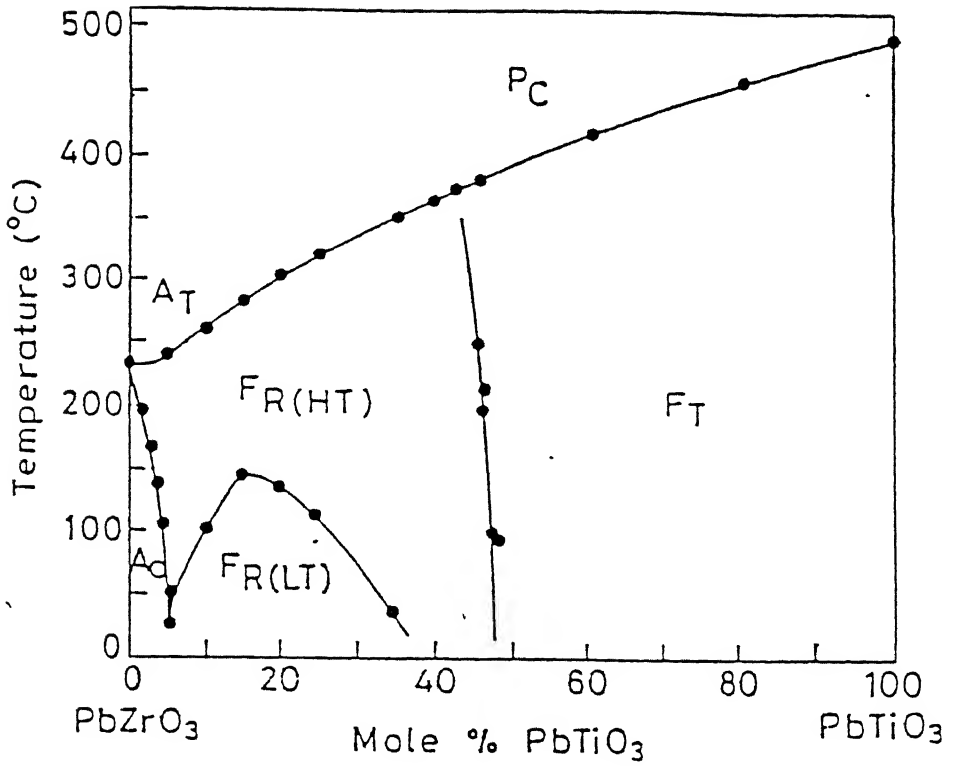


Figure 1.2: The PZT Phase Diagram [after Jaffe et al.(1)]

electromechanical coupling snd dielectric constant are observed for the composition near MPB.

During the phase transition in order to minimize the accompanying stresses, each grain of the ceramic breaks into domains, in a domain the polarization is directed along the crystallographically allowed directions. Because of the random orientations of the domains the net polarization of the sample is zero. However when an electric field is applied to the crystal the domains with polarization components along the applied field direction grow at the expense of the antiparallel domains, thus the polarization increases and finally saturates with further increase in electric field, and the sample attains net polarization (BC) Figure 1.3 . The extrapolation of the linear part BC to the zero electric field gives the spontaneous polarization Ps. When the electric field corresponding to point B is reduced, the polarization of the sample decreases but for zero applied electric field there remains the remanent polarization Pr. The field required to make the polarization zero again is called the coercive field, Ec. The so obtained hysteresis loop is of particular importance for use in ferroelectric memories.

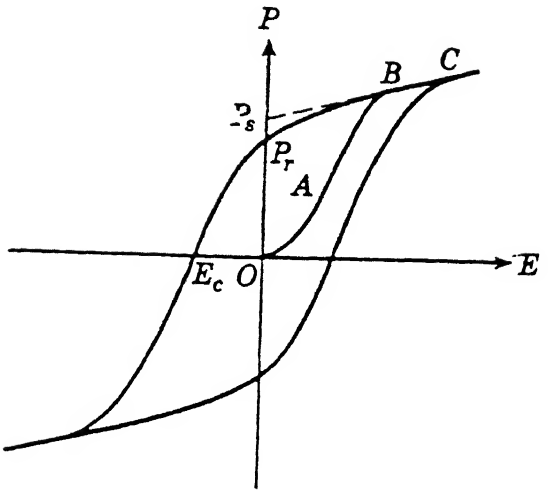


Figure 1.3: Typical Hysteresis Loop of a Ferroelectric Ceramic (Ref.3)

## 1.3 Ferroelectric Thin Films:

Bulk materials both single crystals and ceramics still dominate the research activities in the ferroelectric films research activities are also increasing rapidly . Several phenomena in ferroelectric materials such as polarization hysteresis, pyroelectricity and electrooptic activities are exploited to make integrated devices on semiconductor IC chips eg., the new application for memory and logic circuits on Si or GaAs require the use of thin films. Undoubtedly the thin films provide many advantages over bulk counter parts including the reduced operationg device voltage and the compatibility of the film deposition techniques with establishd silicon microelectronic processing which makes integration with planer circuit technology possible.

## 1.4 Application Of PZT Thin Films:

The various phenomenon like polarization hysteresis, pyroelectricity, peizoelectricity can be exploited to fabricate a number of useful devices eg,. the hysteresis properties of ferroelectric thin film can be used to fabricate the nonvolatile memories. The pyroelectric properties of PZT thin film can be used to develop a sensor for infrared detection. Another application of ferroelectric thin film includes the SAW devices,

ferroelectric gates (FET) and MIST ( Metal insulator semiconductor transistor) etc.

## 1.5 PZT Thin Film In Nonvolatile Memories:

The phenomenon of ferroelectricity readilly lends itself to use in digital systems since the material is able to reside in one of the two different polarization states which may be ascribed to 0 and 1 digital states. In addition the material may be repeatedly switched between states through the application of an electric field. This is exhibited by the hysteresis behaviour of the material when the alternating electric field is applied to it. But when the ferroelectric material is repeatedly cycled from one state to another polarization state its dielectric and ferroelectric properties deteriorate. This phenomena is known as ferroelectric fatigue and is a limiting factor for the performance of memory devices using these materials. During the ferroelectric fatigue, the ferroelectric polarization decreases with increasing switching cycles. This leads to an unacceptable device performance. The entrapment of oxygen vacancies at the ferroelectric-electrode interface is mainly responsible for fatigue (2). It is beleived that oxide electrodes can prove better fatigue resistance because they reduce oxygen vacancy pile up at the interface by exchanging oxygen vacancies with the oxygen in oxide electrode.

## 1.6 Need To Make PZT Films On Silicon:

Use of ferroelectric properties for device application is now well established. The microelectronic applications of ferroelectric thin films have undergone a resurgence recently. Advances are highlighted by the announcement of commercial ferroelectric devices fabricated in conjuction with silicon technology. Coupling of these two materials and fabrication process open a new filed for the application of ferroelectric thin films. Higher device density is achieved by using ferroelectrics in place of $SiO_2$. The high dielectric property of ferroelectric materials allows the reduction from conventional device sizes. Using the ferroelectric property,the potential for high density, fast, nonvolatile and radiation hard devices has been realized.

## 1.7 Problem With Silicon- No Perovskite Phase:

In coupling ferroelectic processing with silicon technology, several new problems arise. One of them is the diffusion of ferroelectric constituents into silicon at the processing

temperatures. Recently Majumder et al (3) have done a detailed study of effect of substrates on the phase formation of PZT thin films. They deposited PZT films of thickness 0.6 $\mu$m on two groups of substrates (a) crystalline ( sapphire, stainless steel, alumina and silicon) (b) Amorphous ( quartz, sodalime and silica glass). The XRD patterns of the films confirm the perovskite phase for all the other crystalline substrates except for silicon and s.s, while all the amorphous and two of the crystalline substrates silicon and s.s yields a pyrochlore phase. Similar results have also been reported by others (4). For device application, the perovskite phase is needed. the pyrochlore phase is paraelectric and its presence degrades the properties.

## 1.8 Need for a Conducting Barrier Layer:

A crucial factor favouring the formation of pyrochlore structure is the deficiency of Pb in the film by the diffusion of Pb into the substrate. However, this can be prevented by interposing a suitable diffusion barrier between the ferroelectric material and silicon substrates. So, a oxide diffusion barrier is required for achieving ferroelectric devices on silicon. This diffusion layer must be conducting to avoid the use of any additional conducting layer for bottom electrode.

## 1.9 Electrodes For PZT Ferrroelectric Thin Films:

For PZT thin film applications, metal electrode such as Au, Pt and Ag are used widely. However, there are several disadvantags in using metal electrodes. In general, ferroelectric films suffer from fatigue on metal electrodes. As mentioned in earlier section the entrapment of defects (oxygen vacancies) at the interface, the large Schottky barrier height that arises due to lattice mismatch and work function difference between the metal electrode and ceramic ferroelectric are beleived to be main causes for the defect entrapment at the interface. Another distinct disadvantage in using platinum electrodes is the difficulty involved in etching the material which is an important consideration in VLSI application.

These considerations have led to the search for alternate electrode materials for PZT thin film applications. To reduce Schottky barrier height at the interface, we must use an electrode material whose work function and lattice parameters are similar to that of the PZT thin films. In previous study, Parikh et al. (5) investigated the use of ceramic nitrides and oxide diffusion barrier such as $ZrN_x$, $TiN_x$, $ZrO_x$, and $TiO_x$ for

PZT thin film applications. But their results indicate imtermixing at low temperatures using these compounds.

Ceramic conductros such as $RuO_2$, ITO and other transition metal oxides eg. $IRO_2$, $RhO_2$, and $ReO_2$ etc are some other choices. The metal oxides of these transition metals tend to crystallize in the tetragonal rutile structure and are promising candidates for various metallization schemes primarily because of their low resistivity and high thermal stablity (6).

## 1.10 Why $RuO_2$ Is Better:

Ruthenium dioxide, $RuO_2$ is one of the few stoichiometric oxides that exhibits metal like conductivity at room temperature, with room temperature bulk resistivity reported in the range of 30 to 100 $\mu\Omega$cm (7). Other important properties of this transition metal oxide include chemical stability at elevated temperatures (7), and excellent diffusion barrier characteristic. The use of this material as electrode in VLSI, therefore obviates the need for an additional barrier layer film. Recently it has been shown that these films can be etched using conventional dry etching techniques (8).

## 1.11 Fabrication Roots For $RuO_2$ Thin Films:

Several fabrication routes for $RuO_2$ thin films have been reported, out of which the common methods are rf sputtering, dc magnetron sputtering, CVD and solution chemistry technique. A solution chemistry technique offers an alternative approach for synthesis of $RuO_2$ thin films. Advantages of this technique includes easy control of composition, low processing temperatures and the ability to fabricate larger area films at relatively low cost.

## 1.12 Work Done On $RuO_2$ Electrode-A Brief Review:

There are few recent reports on the preparation of $RuO_2$ thin film by different methods, its characterization and comparision of $RuO_2$ electrodes with other oxide electrodes and metal electrodes on the electrical properties of PZT thin film. L.K.Elbaum et al(9) reported on resistivity, microstructures and diffusion barrier property of reactively

sputtered films of $RuO_2$. Films of $RuO_2$ of thichness 1500 - 3000$\AA$ were reactively sputtered in a dc magnetron sputtering system using a mixed Ar-$O_2$ atmosphere. Prior to the sputter deposition the system was pumped down to a pressure of $9x10^{-7}$ Torr and presputtered for 1 h with oxygen and argon gases, stabilized to a total pressure of $2x10^{-4}$ Torr. The oxygen content was varied from 0% to 100% of total pressure. The temperature of the wafer during sputtering was $500^0$C, which assured low resistivity of as deposited films. The substrate used was 2 $\mu\Omega$cm (100) oriented p-type silicon and sapphire. RBS and XRD analysis were employed to identify the composition of films and their microstructure was investigated with TEM.

In the XRD pattern they found a large number of diffraction peaks, all of which were identified as pertaining to stoichiometric $RuO_2$. The narrow width of the peaks pointed to a polycrystalline microstructure with medium size grains. Both XRD and RBS analysis confirmed that as deposited $RuO_2$ films remain stoichiometric when the oxygen content is varied from 25% to 100% confirming $RuO_2$ as the only stable oxide of Ru formed.

They have measured the resistivity by four terminal Vander Paw method in standard helium cryostat. The resistivity of a typical $RuO_2$ deposited film with 50% $O_2$ as a function of temperature is shown in Figure 1.4. At room temperature resistivity is about 40 $\mu\Omega$cm. $RuO_2$ behaves like typical metal with resistivity deviating from linear dependence on temperature at about 150 K . The resistivity decreases slightly upon annealing in oxygen, and the shallow resistance is observed after $800^0$C annealed in argon. So the resistivity of $RuO_2$ which is comparable to that of refractory metal nitrides, is too high for application of $RuO_2$ as interconnects, but it is perfectly acceptable for application in VLSI as a contact to a device.

To probe metallurgical interaction with Al they evaporated 1000 $\AA$ Al film over 2000 $\AA$ $RuO_2$ with silicon as substrate. The RBS spectra of an as deposited sample and a sample annealed in argon at $600^0$C confirms that $RuO_2$ is an excellent diffusion barrier between Al and Si in contact metallization. Similarly they found that the Pd/$RuO_2$/Si structure and $RuO_2$ interface with $SiO_2$ and with PtSi is also stable upto $600^0$C.

Vijay and Desu (6) prepared the thin films of $RuO_2$ and ITO and compared them as an electrode material for PZT films. They have deposited the films of $RuO_2$ and ITO by sputtering in oxygen atmosphere at a pressure of $2\times10^{-4}$ Torr on to Si substrates. The substrates were maintained at a temperature of $200^0$C during deposition and the electrode were deposited to a thickness of 500 nm. Sol gel derived PZT thin films then were deposited on these substrates. The PZT precursor was prepared utilising the method proposed by Yi et al.(10) . PZT films were spin coated at 1500 rpm for

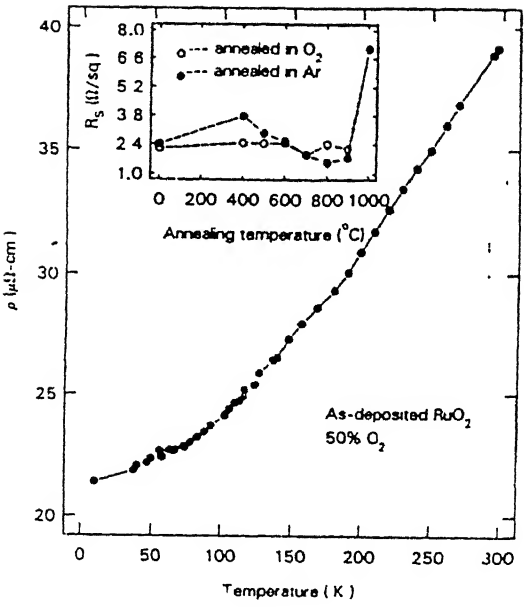


Figure 1.4: Resistivity Vs. Temperature of as Deposited $RuO_2$ 50 %Oxygen(Ref.8)

20 seconds and subsequently dried at $150^0$C for 5 minutes. In a similar study they have deposited PbO films on the electrodes by vaccum evaporation techniques under a vaccum of $10^{-6}$ Torr to a thickness of 150 nm. These coated films were annealed at various temperatures between 400 and $700^0$C for 30 minutes.

The presence of thin film phases and a qualitative estimate of degree of intermixing as a function of annealing temperature were determined from thin film X-ray difraction studies. RBS analysis of the samples were performed to determine the extent of intermixing using a 2 MeV $He^+$ beam reference. Figure 1.5 compares the Pb concentration of PZT films on $RuO_2$ and ITO electrode. At the annealing temperatures up to $550^0$C, there is little difference in the relative Pb concentration in the PZT films on both these electrodes. However, above $550^0$C, the relative Pb concentration in $RuO_2$/ PZT films remains almost constant, while in the ITO/PZT samples the Pb concentration shows a decreasing trend. The RBS spectra obtained on the Si/ITO/PbO samples and Si/$RuO_2$/PbO are shown in Figure 1.6. The spectra of the samples annealed upto $450^0$C are essentially similar to that of as deposited sample. However, the Pb yield has decreased considerably, indicating a loss of Pb atoms from PbO. The drastic increase in the low energy edge of Pb peaks indicates that Pb diffuses into ITO layer. In and Sn diffuse toward the surface and react with PbO to form a Pb-In-Sn compound. In the Si/$RuO_2$/PbO samples, the RBS spectra show lead diffusion towards the electrode

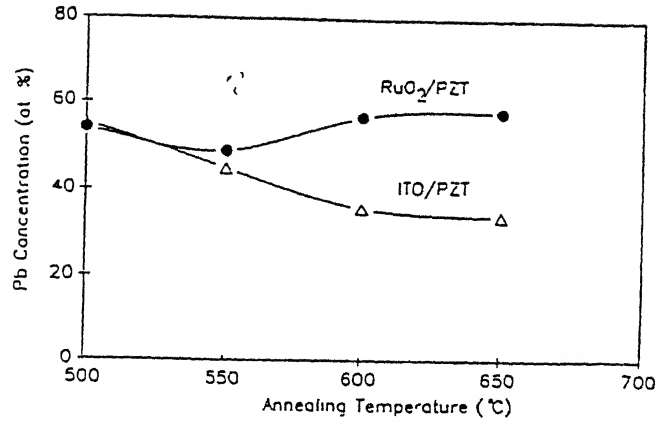


Figure 1.5: Comparision of Pb Concentration on Surface of $RuO_2$/PZT and ITO/PZT Films as a Function of Annealing Temperature(Ref.6)

at and above $550^0$C. There is a tail in the Pb peak that extends toward the lower energies. At higher annealing temperatures, this low energy tail is more prominent . A comparative RBS spectra of Si/ITO/PZT and Si/$RuO_2$/PZT shown in Figure 1.7. It appears that there is no noticiable intermixing between Pb and $RuO_2$. Increased intermixing is observed in the samples annealed at $600^0$C or higher.

Further they reported on the differences in properties of PZT films on metal and ceramic elcetrodes from the fatigue test. Fatigue test was performed under the accelerated conditions using a 1MHz square wave and an electric field of 0.16 mv/cm. The PZT films on Pt electrodes showed early loss of polarization while no fatigue was observed up to $2x10^{+11}$ cycles on $RuO_2$ electrodes.

Their results of dc leakege current measurements on the $RuO_2$/PZT/$RuO_2$ and Pt/PZT/Pt samples are shown in Figure 1.8. The study was conducted at the elevated temperatures ($125^0$C) to obtain stable current level readings. Also, for comparison, only the results of the current flow in one direction(from top to bottom electrode) is plotted in the figure. The films on $RuO_2$ electrode show a lower current level at any particular electric field.

Based on XRD, RBS and electrical characterization studies they concluded that

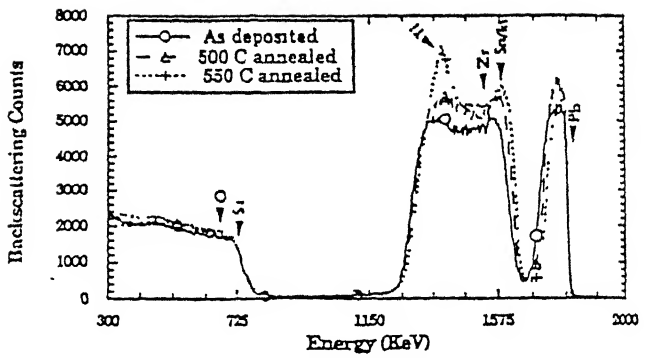


a

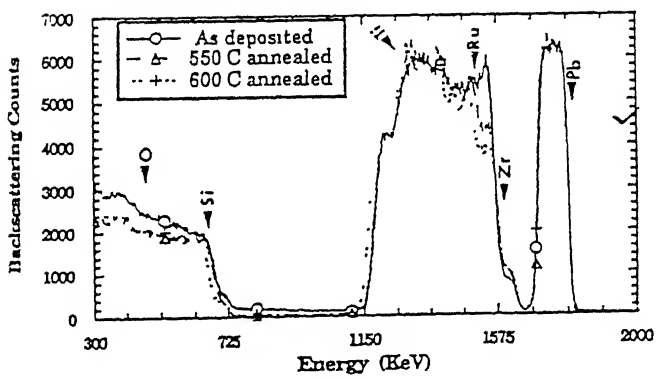


b

Figure 1.6: RBS Profile of as Deposited, 500 and 550$^0$C Annealed (a) Si/ITO/PbO (b) Si/$RuO_2$/PbO Samples(Ref.6)

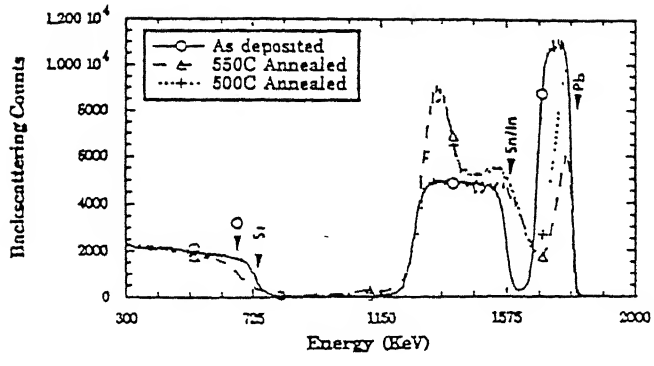


a

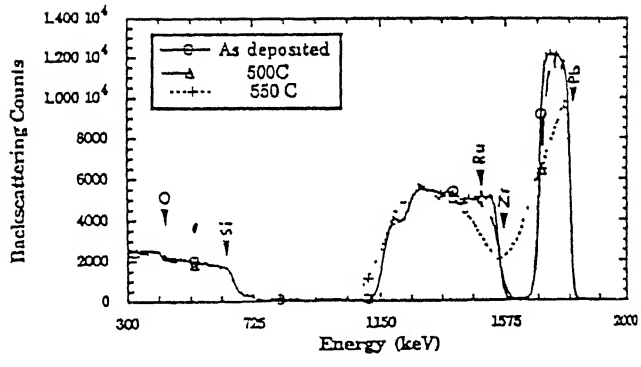


b

Figure 1.7: RBS Profile of as Deposited, 500 and 550$^0$C Annealed (a) Si/ITO/PZT (b) Si/$RuO_2$/PZT Samples(Ref.6)

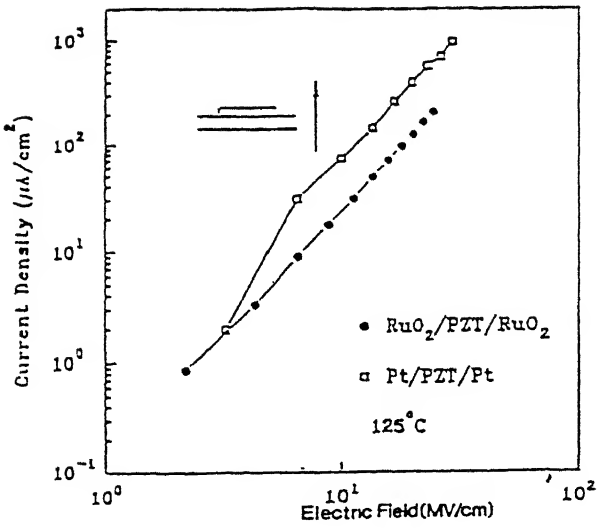


Figure 1 8: Electrode Effects on I-V Characteristics of PZT Films(Ref.6)

$RuO_2$ is a better electrode material for PZT thin film devices compared to ITO. Diffusion barrier properties of various ceramics thin films such as $ZrN_x$, $TiN_x$, $TiO_x$, and $ZrO_x$ were compared with those of $RuO_2$ and ITO. $RuO_2$ is more effective barrier to the interdiffusion of Pb and Si at high temperatures. No intermixing was observed up to the temperatures as high as $600^0$C in $RuO_2$/PZT samples while the intermixing was severe in ITO/PZT samples at temperatures above $500^0$C. It is possible to form the PZT perovskite phase on $RuO_2$ electrodes at temperatures where there is no serious interdiffusion of the constituent elements.

There is one very recent report by Tressler et al.(7) devoted to the synthesis of $RuO_2$ thin film by solution chemistry method. The advantage of this technique includes easy composition control, excellent homogeneity, fine grain size, low processing temperatures, the ability to fabricate large area films and relatively low cost. Tressler et al. deposited the $RuO_2$ thin films by spin coating method. The precursor $RuO_2$ solution was prepared by dissolving appropriate amount of $RuCl_3.nH_2O$ in enough ethanol to prepare 0.38M solution. This solution was coated on Si substrate by spin coating method. Such films spun on to the silicon substrate were fired at various temperatures $400^0$C, $500^0$C, $600^0$C, $700^0$C and $800^0$C. Three different firing times were used to see which one provides the best film. In first schedule each successive layer was fired for 1 hour. In second, each layer was fired for 10 minutes. In the third sample initial layer

Table 1 1: Grain Size, RMS Roughness, and Resistivities of $RuO_2$ Thin Films as a Function Firing Temperature (Measured at 300 K)

| Firing temperature (°C) | Grain size (nm) | Roughness (nm) | Resistivity ($\mu\Omega$ m) |
|---|---|---|---|
| 400 | 30 | 3 4 | 3.1 |
| 500 | 50 | 3.7 | 2.8 |
| 600 | 120 | 7.9 | 2.8 |
| 700 | 200 | 11 | 2.1 |
| 800 | 250 | 14 | 1.8 |

was fired for 10 minutes with successive layer fired for 2 minutes. Various characterization of these films eg. XRD, grain size, film thickness and resistivity determination etc. were performed.

The XRD patterns of the samples fired at different temperatures indicate that the crystallisation of $RuO_2$ starts at about $400^0$C and reaches a maximum at $460^0$C. The crystallization of $RuO_2$ film is effectively complete after $600^0$C. Further on the basis of SEM analysis they have reported that short firing times eg. 2 minutes firing suppresses the grain growth so that a fine, equi-axed and uniform grain size is achieved. However, with longer firing times some larger grains grow at the expense of smaller grains, resulting in the formation of crater like film surface. These results suggest that the first layer applied to the silicon substrates plays an important role for the successful crystal growth of the successively applied layers. The first layer is seed layer of the following layers. If the quality ie the crystallinity, grain size etc of this seed layer can be optimized, then the total performance of film can be enhanced.

They measured the resistivity of the $RuO_2$/Si system using conventional four point probe technique. For making good contact on $RuO_2$ film they deposited Gold strips between 1 and 2 mm wide and 200 nm thick. Wire leads were attached to the gold electrodes using air dried silver paste. The Table 1.1 shows the average grain size, resistivity and RMS roughness of the $RuO_2$ thin films as a function of firing temperature. These data show that as the crystallinity and the average grain size of the film increses the resistivity decreases. Since no Ruthenium metal was observed in any of the XRD patterns, one can conclude that the firing temperature dependence of the resistivity

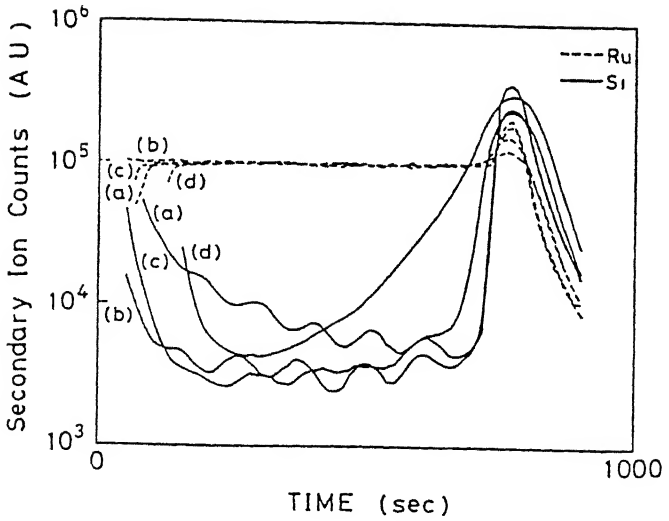


Figure 1.9: The SIMS Depth Profile for 7 Layer Thick $RuO_2$ Films a to d correspond to Films Fired at 400, 500, 600, and 700$^0$C(Ref.7)

is associated not with mixing of Ru metal and $RuO_2$ but rather with the grain size, crystal imperfections specially in the grain boundary region and film porosity.

The SIMS depth profile of the $RuO_2$/Si films fired at 400$^0$C, 500$^0$C, 600$^0$C and 700$^0$C are shown in Figure 1.9. The boundary between $RuO_2$ films and Si substrate was very sharp upto the firing temperature of 500$^0$C. The inter-diffusion of the elements at $RuO_2$/Si interface begins when the firing temperature exceeds 500$^0$C. Above 700$^0$C, the silicon diffusion of $RuO_2$ film was very serious.

So according to Tressler et al short firing times at temperatures between 500$^0$C and 700$^0$C are critical for controlling the grain growth. In addition, these short firing times appear to have no significant effect on the formation of crystalline $RuO_2$. Lastly, the resistivity of the film can be tailored to fit a particular application by simply changing the firing temperature of the film.

## 1.13 Aim of Work:

From the review it is clear that there has been very little study on the preparation and characterization of $RuO_2$ thin films on Si substrates by solution chemistry method, and almost no work on the preparation and characterization of PZT thin film on $RuO_2$

coated Si by sol-gel method.

In this work our aim is the process optimization for preparation of good quality $RuO_2$ thin film by solution chemistry technique ie the preparation of $RuCl_3.nH_2O$ precursor solution, identification and optemization of the processing parameters required to obtain smooth, crack free, and good conductivity $RuO_2$ films repeatedly on Si substrates. After that preparation and characterization of PZT thin film on $RuO_2$ coated Si substrate using sol-gel method.

# Chapter 2

# Experimental Procedures

In this chapter we have described the experimental procedures used in the present work. First we describe the details of $RuO_2$ film preparation which includes preparation of precursor solution, substrate preparation , film deposition and heat treatment of the film. Then we describe the details of characterization procedures used during the course of work including XRD , Scanning Electron Microscopy , Four Probe Vander Paw method of resistivity determination, Rutherford back scattring spectrometry (RBS) After that we describe the details of PZT/$RuO_2$/Si system preparation including Preccusor sol preparation , film deposition and heat treatment. At the end various characterization procedures of the PZT/$RuO_2$/Si system have been described.

## 2.1 $RuO_2$ Thin Film Preparation:

### 2.1.1 Preparation of Precursor Solution:

All the $RuO_2$ films prepared during the course of this work were prepared using solution chemistry technique. The solution for the film deposition was prepared using the procedure given by Tressler et al (7). We have dissolved approximetly 0.001 moles ie, 0.21 grams of $RuCl_3.nH_2O$ (40% Ru approx., ARORA MATTHEY LIMITED, INDIA) in enough ethanol to make 10 ml of solution of strength 0.1 moles/ litre. The $RuCl_3.nH_2O$ solution in ethanol was mixed at room temperature for atleast 2.0 hours then filtered using 0.5 micron filters. the solution is dark brown in colour and should be prevented from moisture.

## 2.2 Preparation of Substrate:

Single crystal ¡100¿ silicon wafers of high resistivity in the form of $1 \times 1 cm^2$, were used as substrate in this work. Prior to film deposition if necessary the silicon substrates were polished mechanically using velvet cloth and $1\mu m$ and $0.3\mu m$ $Al_2O_3$ particle dispersed in water. The polishing is continued till the mirror finish is obtained. The polishing removes pin-holes, grooves and surface imperfections which may lead to poor quality film.

All the polished substrates were cleaned using ultra-sonic bath in different solutions. The substrates were first ultra-sonicated in soap solution then they were ultra-sonificated successively for five minutes each in triple distilled water, acetone, trichloroethylene, acetone again, triple distilled water again and absolute alcohol and then dried by using tissue paper.

## 2.3 Film Preparation:

The ruthenium dioxide precursor solution was coated on the substrates by spin coating technique. A research centrifuge (Remi instruments, India) with variable rpm was used as spin -coating unit. The substrate was fixed at the centre of head of centrifuge using double-sided tape and rotated at about 4000 rpm. At this rpm of substrate a drop of solution was put on the substrate using a glass syringe. The drop of solution immediately spreads on the substrates and uniform film is obtained. The spinning time was selected as 10 seconds.

The thickness of the film obtained in the single coating is mainly controlled by strength of solution and spin speed. The film thickness linearly increases in proportion to the increase in molar concentration of the solution. This film thickness can also be controlled by the spin speed. The relationship is given by the equation:

$$t = kw^m \tag{2.1}$$

where,
t =film thickness
k = constant dependent on evaporation rate and molecular weight of the solvent,
n = some constant ,
w = spin speed in rpm.
Multiple coatings are carried out to get desired thickness of $RuO_2$ film.

## 2.4 Heat Treatment Of Films:

The thin film spun on to the silicon substrates were fired in a quartz tube furnace controlled by a controller. A chromel-alumel thermo-couple is used to sense the temperature close to sample. The samples were inserted in the furnace tube using a quartz boat. After holding the sample in the furnace for required time the sample is quenched to room temperature.

The firing schedules used in this work are similar as proposed by Tressler et al []. In first schedule the thin films were fired at temperatures of either $400^0$C, $450^0$C, $500^0$C, $550^0$C. $600^0$C,or $700^0$C with first layer fired for 10 minutes and each additional layers fired for 2 minutes. In second schedule the samples were fired at a fixed temperature of $500^0$C and $550^0$Cwith different firing times with either first layer fired for 10 minutes and rest layers for 2 minutes or first layer fired for 10 minutes with each additional layer for 5 minutes or all the layers fired for 10 minutes.

## 2.5 Characterization Of $RuO_2$ Thin Film:

### 2.5.1 Optical Microscopy:

After preparation of films of desired thickness they are examined in a optical microscope (Carl Zeiss, Germany) to detect presence of eyelands or cracks. Presence of eyelands in the film may give absurd resistivity data.

## 2.6 X-Ray Diffraction Study:

The X-Ray diffraction technique has been used to analyse the phases. Phase analysis was carried out on all the $RuO_2$/Si films. The XRD patterns were recorded using X-Ray diffractometer (Rich Seifert Iso-Debyflex 2002, Germany). CuK$\alpha$ radiation is used with Ni monochromator. Operating parameters of X-Ray Diffractometer selected for this work are tabulated below:
Accelerating voltage = 30 KV
Accelerating current = 20 mA
Scanning speed = $3^o$/min.
Chart Speed = 3 cm/min.
Counts per minute = 5K

Time constant = 10 s
The XRD pattern of the sample are recorded in a $2\theta$ range from $20^0$C to $60^0$C.

## 2.7 Scanning Electron Microscopy:

The scanning electron microscope (JSM 840 A, JEOL, JAPAN) is used to study the presence of cracks, eyelands etc. in the film as well as the grain size and other micro-structural features. Since the $RuO_2$ film is conducting so it can be observed directly under SEM. For non-conducting films some conducting layer is deposited on the film surface to suppress electron charging effect. The grain size and grain distribution is measured using SEM. The negative is directly displayed on the monitor.

## 2.8 Resistivity Measurement:

The electrical resistance of the $RuO_2$ film was measured at room temperature using conventional four point probe technique. The four point resistivity probe (Model A-4, 1.5 mm., OSAW INDIA) equipped with a dc current source (Model 6181C, H.P.) and a voltage for resistivity measurement.

The theoretical foundation of measurement on irregularly shaped samples is based on conformal mapping developed by Vander Paw (12). The resistivity of flat samples of arbitrary shape can be measured without knowing current pattern if the following conditions are met:

- Contacts are at circumference of sample.
- Contacts are sufficiently small.
- The sample is uniformally thick.
- Sample does not contain any isolated holes i.e. sample is singly connected.

  If a flat sample of arbitrary shape of conducting material with contacts 1, 2, 3 and 4 along the periphery, satisfies above conditions then, the resistance $R_{12,34}$ is defined as :

$$R_{12,34} = \frac{V_{34}}{I_{12}} \tag{2.2}$$

where the current $I_{12}$ enters the sample through contact 1 and leaves through contact 2 and $V_{34} = V_3 - V_4$ is the voltage difference between the contacts 3 and 4. The resistance $R_{23,41}$ is defined similarly. The resistivity is then given by:

$$\rho = \frac{\pi t}{\ln 2} \frac{R_{12,34} + R_{23,41}}{2} F \tag{2.3}$$

where F is a function of only the ratio $R_r = R_{12,34}/R_{23,14}$, satisfying relation,

$$\frac{(R_r - 1)}{(R_r + 1)} = \frac{F}{\ln(2)} ar\cosh(\frac{exp(\frac{\ln(2)}{F})}{2}) \tag{2.4}$$

For the symmetrical samples such as a circle or a square, $R_r = 1$ and $F = 1$. This allows resistivity equation to be simplified to give resistivity as :

$$\rho = \frac{\pi t}{\ln(2)}(R_{12,34}) = 0.4532 t R_{12,34} \tag{2.5}$$

and sheet resistance is given by:

$$\rho_s = \frac{\rho}{t} = \frac{\pi}{\ln(2)} R_{12,34} = 0.4532 R_{12,34} \tag{2.6}$$

provided $t \leq S/2$
where t is sample thickness and S is probe spacing. In our case the symmetrical shaped square samples are used and the condition $t \leq S/2$ is fully satisfied.

## 2.9 Rutherford Back-scattering Spectrometry:

The RBS has been used for quantitative analysis of film composition, determination of film thickness and also for depth profile analysis. Figure 2.1 shows the details of RBS chamber. The chamber is connected with a diffusion pump system with liquid nitrogen trap. The vaccuum in the RBS is of the order , and can be introduced in the path of 4 $He^{+4}$ beam. The collimated beam of 4 $He^{+4}$ has beam size of about 1 mm. square. The detector is mounted at a scattering angle $\theta$ of 150° and subtends a solid angle of about 2.9 mrad at the centre of beam spot. The electrical signals from the surface barrier Si detector are analysed using standard nuclear electronics and multi- channel analyser (MCA). The height of the signal gives energy of detected particles . A plot of energy of the particles Vs. frequency of occurrence of the signals is called spectra. In this measurement an EG & G ORTEC 142A pre-amplifier and PC based MCA are used.

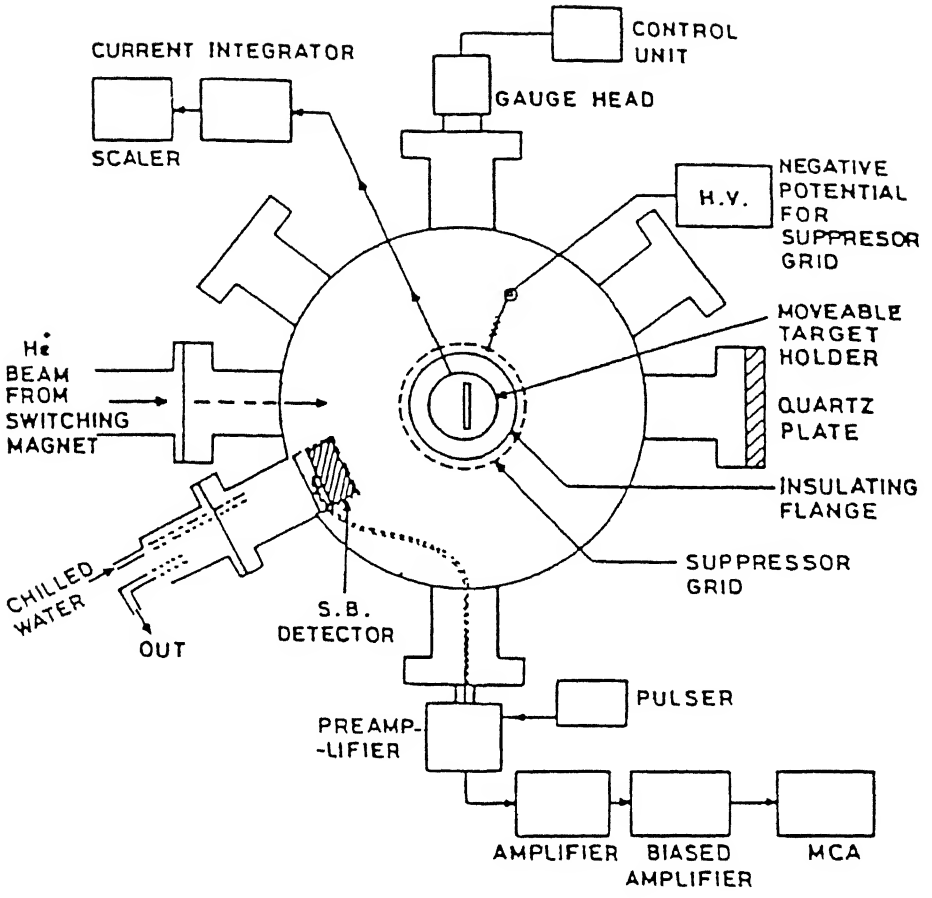


Figure 2.1: Schematic of RBS Chamber

In this work the program developed at the Cornel University by Doolittle (11) called RUMP has been made use of to analyse RBS spectra. In this simulation a theoretical sample structure consisting of several layers of varying thickness is first prepared . A back scattering spectrum is then constructed using the sample structure and experimental parameters. This theoretical profile is then compared with the experimentally observed RBS spectrum. This procedure is utilised in an iterative manner to arrive at the best set of parameters in the simulation structure using which the simulated spectrum compares almost exactly with the experimental spectrum.

## 2.10 Preparation and characterization procedure of PZT thin film on $RuO_2$/Si system:

### 2.10.1 Introduction:

As mentioned earlier, the $RuO_2$ films were prepared by the solution chemistry method and the advantages of solution chemistry techniques were highlighted. Till now we have not seen any work on the preparation of PZT thin film on the $RuO_2$/Si system (by solution chemistry technique) using sol-gel method. In the present work after optimizing the preparation conditions of $RuO_2$ films we have made an attempt to prepare PZT thin film on the $RuO_2$/Si system by sol-gel method. In this section we have described the experimental procedure used in the preparation and characterization of PZT/$RuO_2$/Si system.

## 2.11 Sol-Gel method:

The sol-gel technology provides a method of fabrication of high quality ceramics and glasses. The term sol represents the solution of submicron particles and gel represents the interconnected porous mass obtained from the sol. In the recent years, this technique has been extended to fabrication of thin films or coatings on different substrates. In particular, it has been used extensively in production of films of materils such as ferroelectric PZT, high temperature super conductor yttrium-barium copper oxide, conducting coatings such as indium-tin-oxide, and optical and protective coatings of complex oxides.

Table 2.1: Chemicals Used in the Present Work

| & Chemicals | Moles |
|---|---|
| Lead acetate | 1.05 |
| Acetic acid | 6.60 |
| Zirconium-n-propoxide | 0.53 |
| Titanium-4-butoxide | 0.47 |

## 2.12 Precursor:

The precursor solution with Zr:Ti = 53:47 for the preparation of the films proposed by Majumder et al (3). The starting materials for the preparation of sol are lead acetate, zirconium-n-propoxide, titanium-4-butoxide and acetic acid. The acetic acid is used as a chelating element to increase the self life of the precursor solution. The relative amounts of various chemicals used in a typical sol are given in table. A 5 mole % of excess lead loss was used to compensate for any lead loss during the heat treatment cycle.

To prepare films a small amount of stock solution was taken and diluted by mixing calcualted amount of propanal and acetic acid to get the strength of 0.25 moles/ litre. Flow diagram of precursor preparation is shown in Figure 2.2.

## 2.13 Spin Coating of PZT Thin Film:

The $RuO_2$/Si substrates are coated with PZT sol using spin coating technique. The substrate is fixed on the head of centrifuge and rotated at 5000 rpm and drop of precursor is applied to it and substrate is kept at 5000 rpm for 5 seconds. The uniformity of the film thickness of the film obtained in the single coating of the solution and spin speed. Multiple coatings are carried out to get increased thickness.

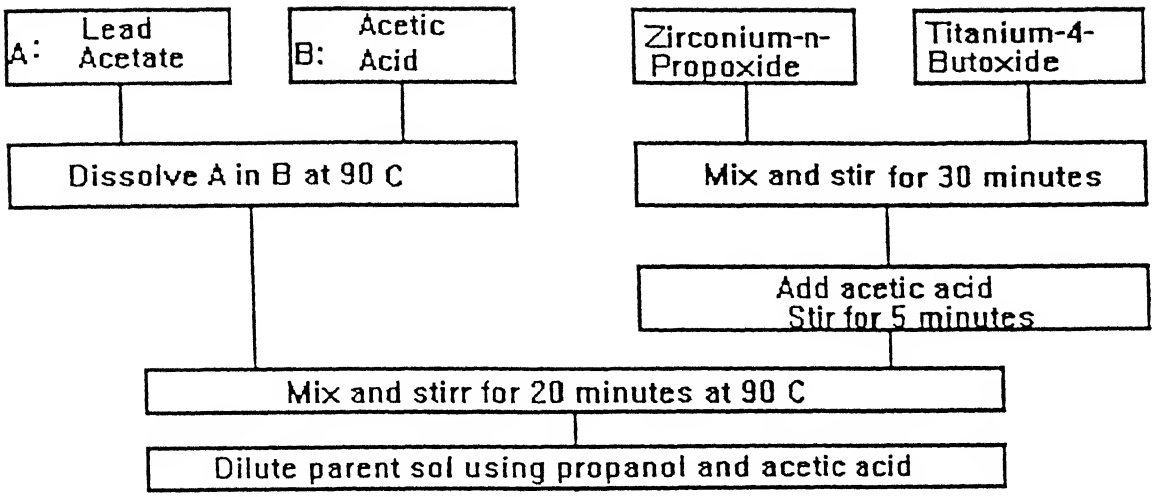


Figure 2.2: Flow Diagram of Precursor Solution Preparation

## 2.14 Firing and annealing:

The firing schedule used for PZT thin films is similar to that proposed by Majumdar et al(3). The films after deposition are fired at $400^0$C for 10 minutes for removal of organics and then quenched to room temperature. Here we have selected firing time as 10 min since longer firing times might increase the resistivity to higher value. Finally the films are annealed at $700^0$C for 2 minutes in air and then quenched to room temperature. Here again the short annealing time is chosen to avoid intermixing of constituents of $RuO_2$ and PZT which is most probable at higher temperatures and could lower the conductivity of $RuO_2$ film. To study the effect of $O_2$ ambient on the phase formation behaviour of PZT films the films were annealed for 2 minutes in $O_2$ ambient in place of air.

## 2.15 Characterization of PZT/$RuO_2$/Si System:

### 2.15.1 Phase Analysis:

The XRD technique has been used to analyze the phases, to determine the crystal structure and to determine the interplaner spacing of phases present. The XRD patterns (Intensity Vs. $2\theta$) of samples are recorded from 20°C to 80°C. The operating conditions are same as mentioned in section 2.6.

### 2.15.2 Miro-Structural Analysis:

The scanning electron microscopy is used to see grain size, grain distribution and other microstructural features of the film as well as to study the presence of cracks, voids etc. in the film. The same procedure and machine are used for this work as mentioned in 2.7.

# Chapter 3

# Measurements, Results And Discussions

## 3.1 Sample Details:

The $RuO_2$ thin films used in this work are prepared by solution chemistry technique. To study the effect of firing schedule on the properies of $RuO_2$ thin films two differents heat treatment schedules are used. In the first set of samples the firing time of the samples is same while firing temperatures are different (isochronal heat treatment) and in the second set of samples the firing temperature is same but firing time is different (isothermal heat treatment).

The first set of samples contains $RuO_2$ thin films on silicon substrate fired at temperatures of $400^0$C, $450^0$C, $500^0$C, $550^0$C, $600^0$C,and $700^0$C with first layer fired for 10 minutes and subsequent layers fired for 2 minutes each. In the second set of samples $RuO_2$ films are fired at $500^0$C and $550^0$C with first layer fired for 10 minutes and subsequent layers fired either for 2, 5, or 10 minutes each. Films of different thickness with fix firing schedules are also prepared to study the effect of film thickness on the conductivity of the film.

## 3.2 Phase Analysis of $RuO_2$ Thin Films:

The X-ray diffraction patterns of $RuO_2$ thin films fired at (a) $400^0$C, (b) $450^0$C, (c) $500^0$C, (d) $550^0$C, (e) $600^0$C, and (f) $700^0$C are shown in Figure 3.1. In each

Table 3.1: X-Ray Diffraction Data of $RuO_2$ Phases

| $2\theta$ | h k l | Int. |
|---|---|---|
| 28.019 | 1 1 0 | 100 |
| 35.066 | 1 0 1 | 77 |
| 40.041 | 2 0 0 | 19 |
| 40.548 | 1 1 1 | 5 |
| 45.021 | 2 1 0 | 1 |
| 54.267 | 2 1 1 | 54 |
| 57.923 | 2 2 0 | 13 |
| 59.491 | 0 0 2 | 7 |

case films were spun at 4000 rpm for 10 seconds, with first layer fired for 10 minutes and remaining layers fired for 2 minutes each. The intensity peaks at an angles $2\theta = 28.02^0$, $35.1^0$, $40.05^0$, and $54.3^0$ confirm the formation of $RuO_2$. Thf X-ray diffraction data of $RuO_2$ phases (JCPDS file 1996) are given in Table 3.1.

As shown in Figure 3.1 the X-ray diffraction peaks of film fired at $400^0$C are poor, showing very little crystallization at this temperature. The X-ray diffraction peaks for the film fired at $450^0$C are neither very ~~very~~ intense nor very sharp. At $500^0$C both the sharpness and the intensity of peaks have increased. After $500^0$C there is basically no change in the peak intensity, since the crystallization is effectively completed at around $500^0$C. These results on thin films are consistent with the previously reported thermal analysis on the sol-gel derived $RuO_2$ particles (13) where crystallization begins at about $400^0$C and a maximum rate of crystallization is acheived at $460^0$C.

It is noticeable in these patterns that above a processing temperature of $550^0$C, there is a slight broadening of the $RuO_2$ peaks. This may be due to intermixing of elements at $RuO_2$/Si interface above this temperature.

Further the firing times for the second and subsequent layers (ie, 2 minutes, 5 minutes, and 10 minutes) with first layer fired for 10 minutes in each case, at a firing temperature of $550^0$C have no significant effect on phase formation of $RuO_2$ films. A little broadening of peaks at 10 minutes firing may indicate the intermixing at interface Figure 3.2.

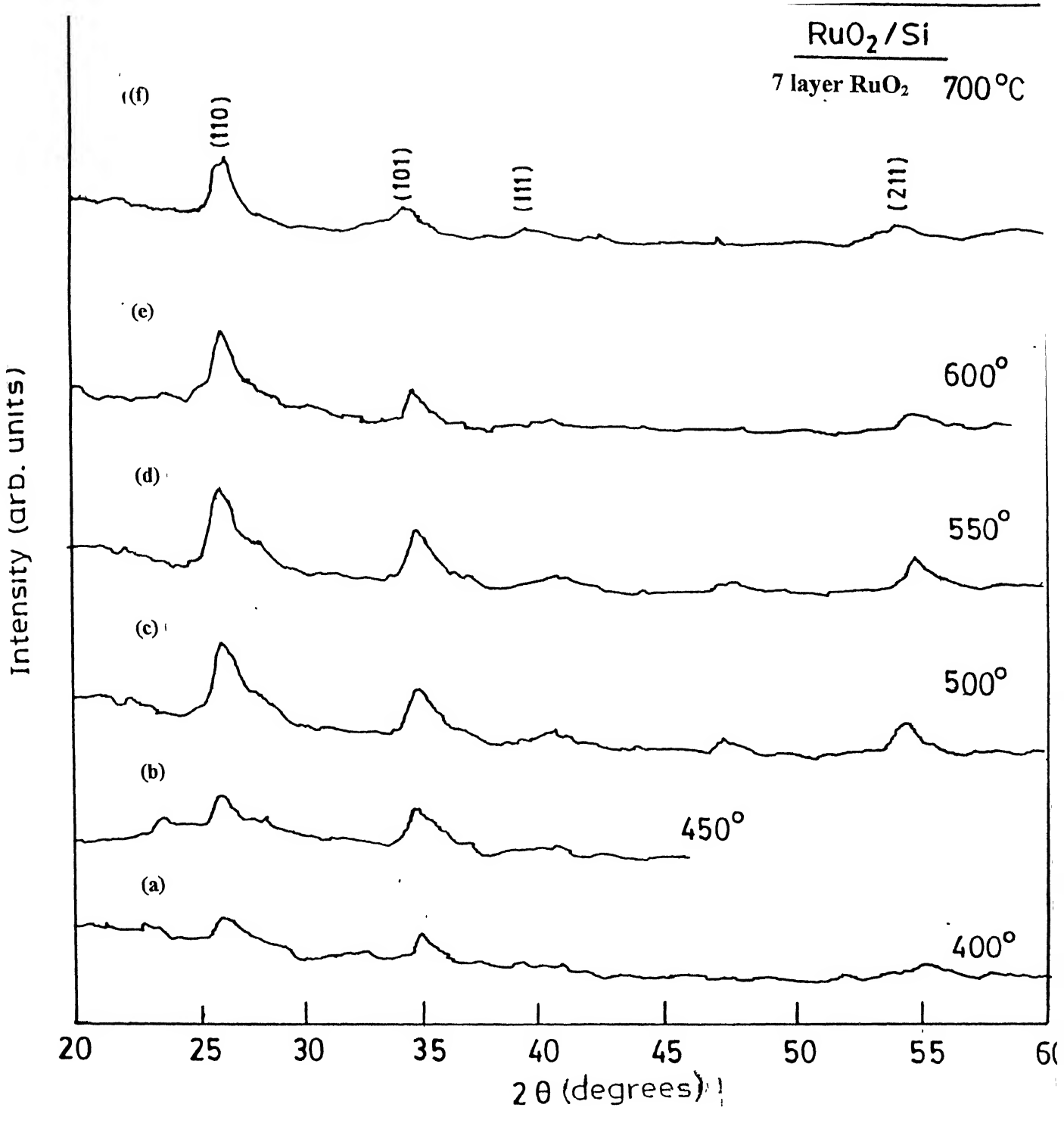


Figure 3.1· X-Ray Diffractograms from $RuO_2$ Films Fired at (a) 400 (b) 450 (c) 500 (d) 550 (e) 600 (f) 700$^0$C with first layer fired for 10 min. and subsequent layers for 2 min.

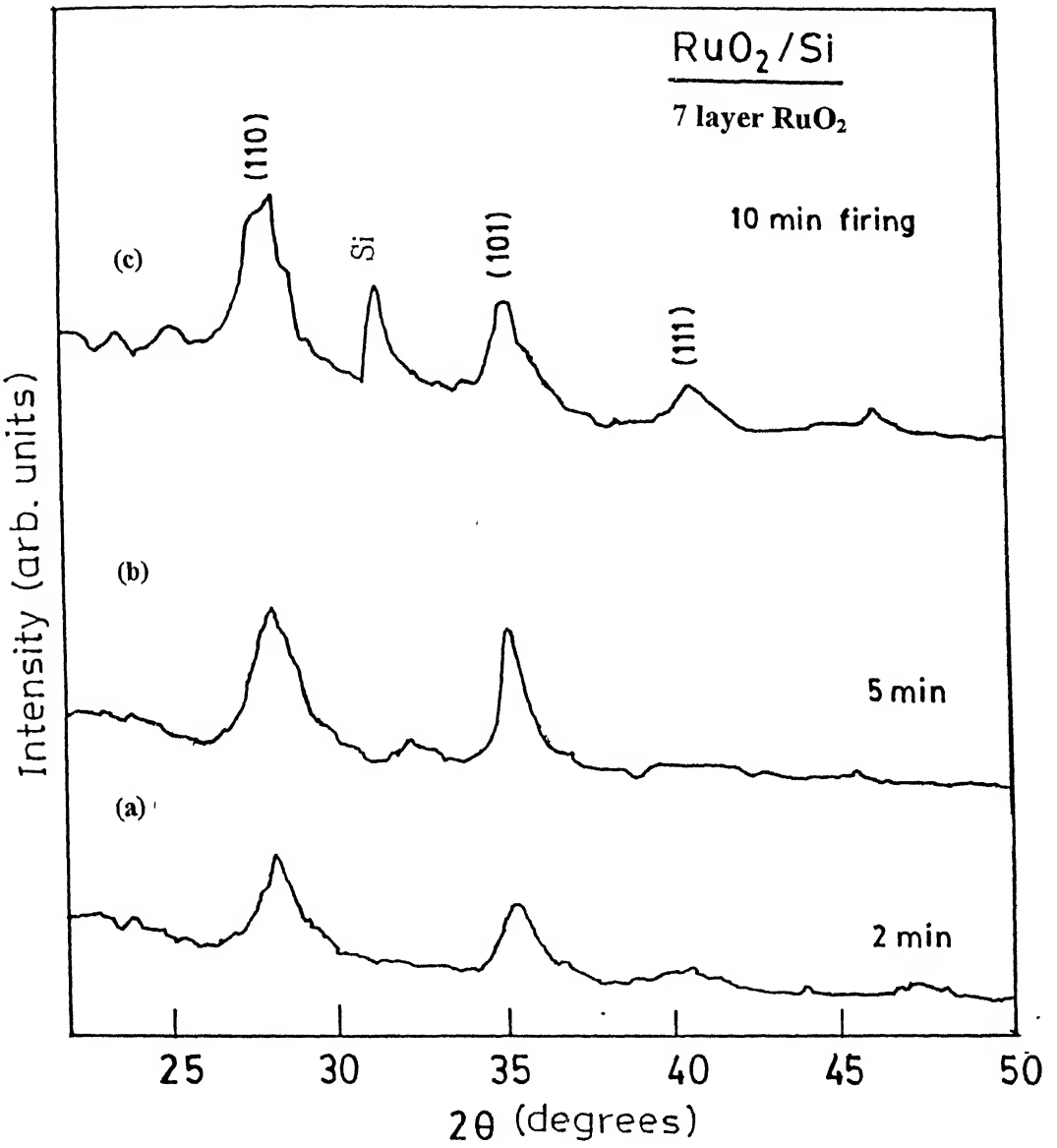


Figure 3.2: X-Ray Diffractograms from $RuO_2$ Films Fired at $550^0$C for (a) 2 min. (b) 5 min. (c) 10 min. with first layer fired for 10 min.

## 3.3 Microstructural Study of $RuO_2$ Thin Films:

The scanning electron micrographs of various samples are shown in Figure 3.3 and 3.4. Figure 3.3 shows the micrographs of $RuO_2$ films fired at various temperatures with constant firing time of 10 minutes for first layer and 2 minutes for rest of the layers.

As seen no grains are observed at $400^0$C. At this temperature the crystallization is in early stage (X-ray diffractographs, Figure 3.1). At $500^0$C very fine grains appear with non-uniform grain size. As the firing temperature is increased grain growth is observed. At $550^0$C fine grains with uniform grain size are observed. At $700^0$C fine grains with some pores are observed. The grain growth also occurs normal to the film surface so that the film surface becomes increasingly rough. The protruding grains give a brighter contrast than others (Figure 3.3 c & d)

Figure 3.4 shows the micrographs of 5 minutes and 10 minutes fired films, with first layer fired for 10 minutes. As can be seen the grain size and the surface roughness of the film increases on increasing the time from 2 minutes to 5 minutes (Figure3.4 a & b). On increasing the time 10 minutes large isolated crystals appear. Similar micrographs are reported by Tressler et al (7) who have verified by EDX that these crystals are $RuO_2$.

## 3.4 Measurement of Sheet Resistance of $RuO_2$/Si Films:

The measurement of sheet resistance is performed on both the categories of samples to see the effect of firing time, firing temperature, and thickness of film on the sheet resistance of the $RuO_2$ thin films.

## 3.5 Effect of Firing Temperature on Sheet Resistance of $RuO_2$ Films:

The sheet resistance of the 7 layered $RuO_2$ films fired at various temperatures with first layer fired for 10 minutes and the remaining layers for 2 minutes is

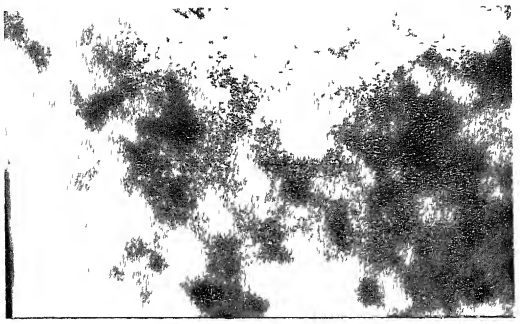


(a)

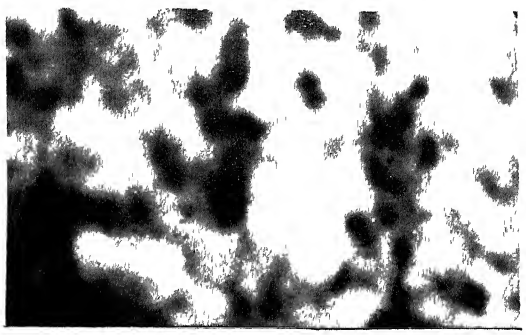


(b)

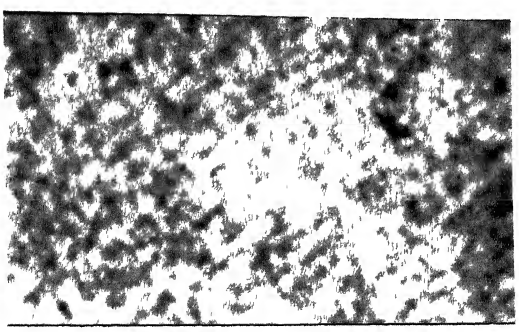


(c)

Figure 3.3: 1 Micro-structures of $RuO_2$ Films Fired at (a) 400 (b) 450 (c) $500^0$C with first layer fired for 10 min. and subsequent layers for 2 min.

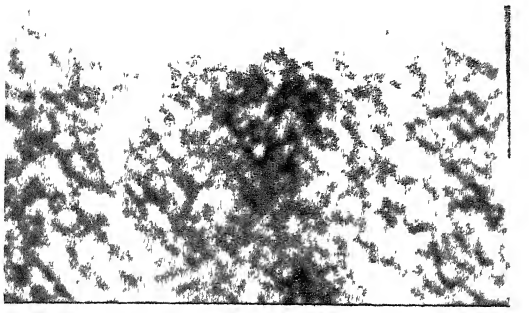


(d)

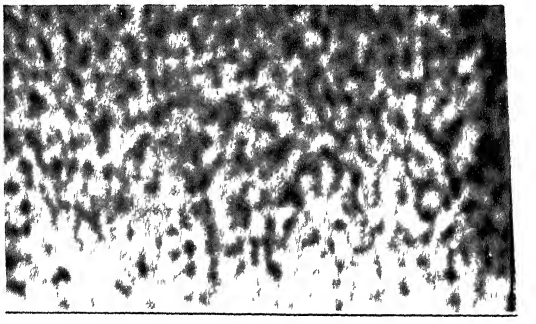


(e)

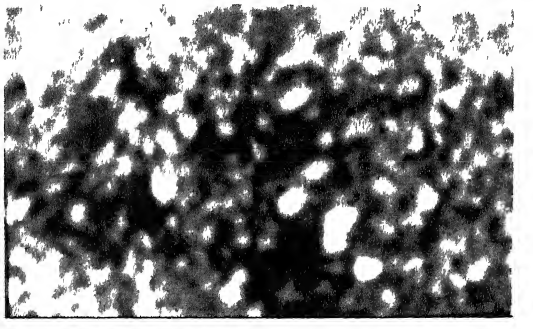


(f)

3.3 Micro-structures of $RuO_2$ Films Fired at (d) 550 (e) 600 (f) $700^0$C with first layer fired for 10 min. and subsequent layers for 2 min.

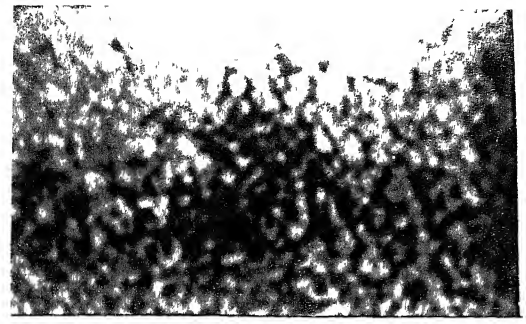


(a)

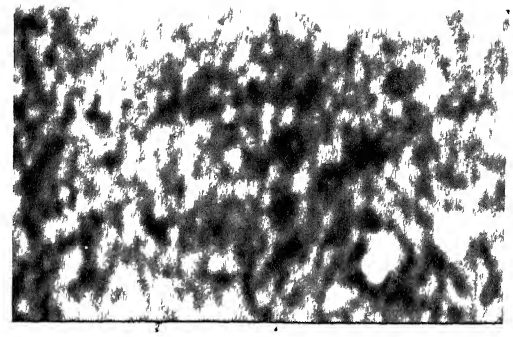


(b)

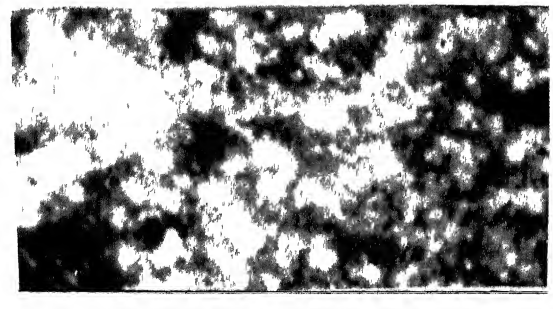


(c)

Figure 3.4: Micro-structures of $RuO_2$ Films Fired at $550^0$C for (a) 2 min. (b) 5 min. (c) 10 min. with first layer fired for 10 min.

Table 3.2: Sheet Resistance of 7 Coatings $RuO_2$ Film at Various Temperatures.

| Temp. ($^0$C) | Sheet resistance (ohm/sq.) | | |
|---|---|---|---|
| | min. | mean | max. |
| 400 | 12.32 | 12.55 | 13.00 |
| 450 | 9.21 | 9.52 | 9.89 |
| 500 | 7.01 | 7.25 | 7.67 |
| 550 | 7.39 | 7.79 | 7.98 |
| 600 | 13.11 | 13.49 | 13.78 |
| 700 | 20.12 | 20.30 | 20.76 |

tabulated in Table 3.2, and Figure 3.5 shows its variation with firing temperatures. From Figure 3.5 it is observed that initially the sheet resistance decreases up to a temperature of 500$^0$C. A dip in the sheet resistance is observed at 500$^0$C and value of sheet resistance remains constant upto 550$^0$C and after that it is increasing again.

High value of sheet resistance at 400$^0$C and 450$^0$C is the result of coexistance of amarphous and crystalline phases of $RuO_2$. After 400$^0$C the decrease in sheet resistance upto 500$^0$C and after that approximately constant value up to temperature 550$^0$C indicates that crystallinity of $RuO_2$ is increasing upto 500$^0$C and is effectively completes at 500$^0$C. These results are in agreement with the results obtained from phase analysis. After 550$^0$C the continuous increase in the sheet resistance with firing temperature may be due to the following reasons:

- Intermixing of elements at $RuO_2$/Si interphase ie, the Si is diffusing in to $RuO_2$ film and thus its resistivity.
- Film shrinkage at high temperatures which results in decrease in the film thickness at higher temperatures thus enhancing the sheet resistance.
- Loss of $RuO_2$ at higher temperatures by the diffusion of Ru in to Si substrate and evaporation of $RuO_2$.

The relative importance of these factors is assessed from further measurements described later.

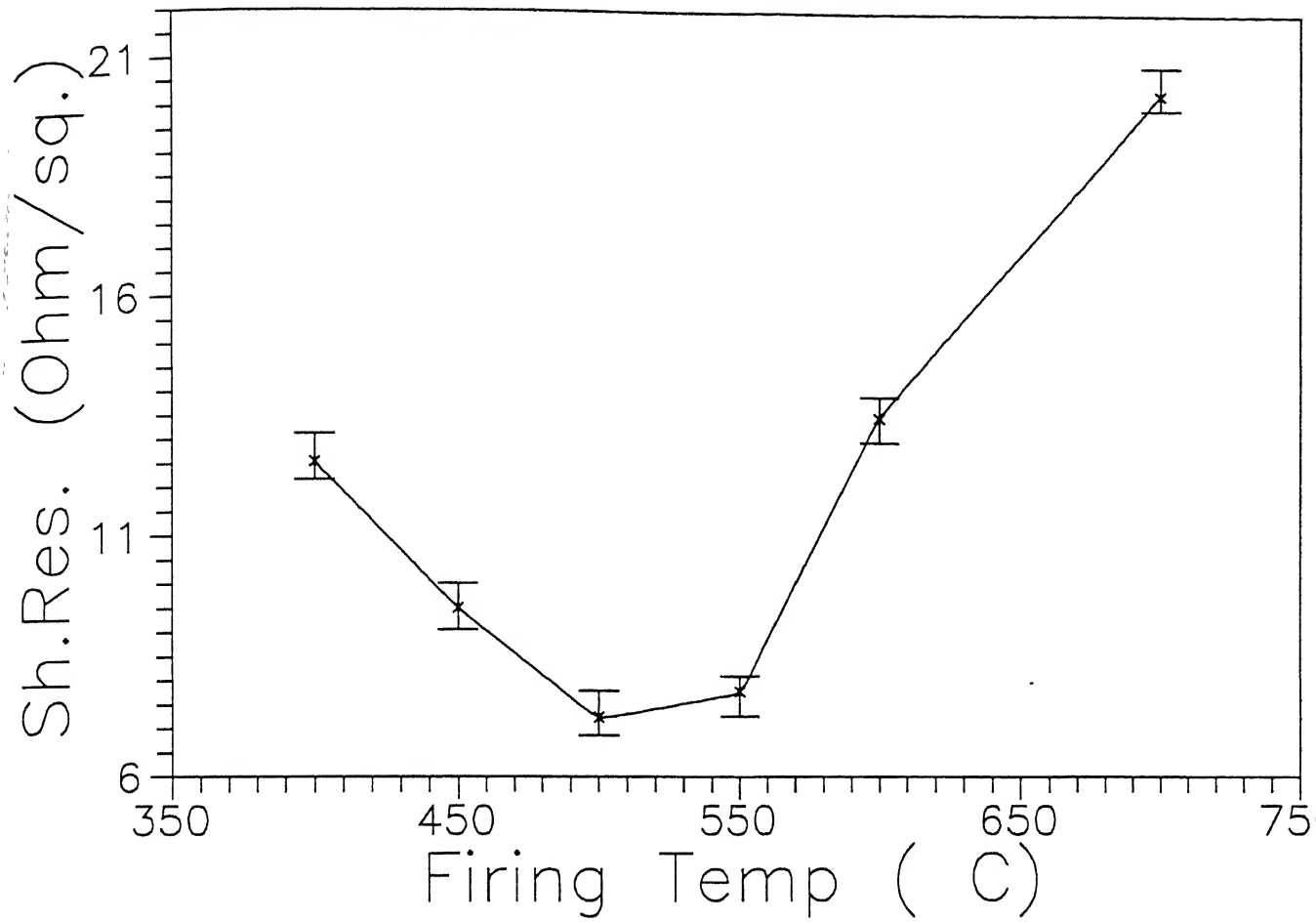


Figure 3.5: Variation of Sheet Resistance with Firing Temperature for $RuO_2$ film with 7 Coatings(First layer 10 min., others 2 min.)

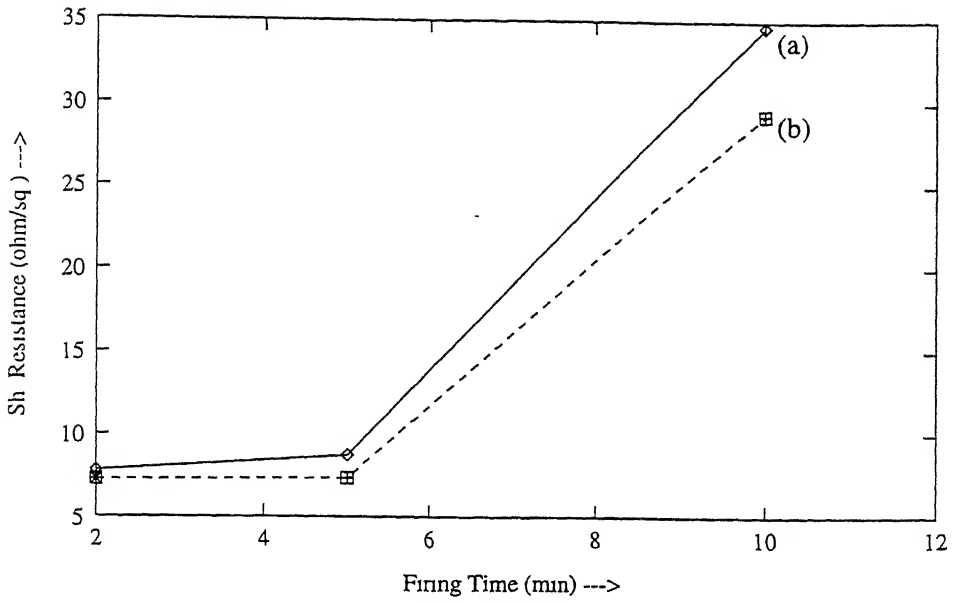


Figure 3.6: Variation of Sheet Resistance with Firing Time at Temperatures of (a) $500^0$C (b) $550^0$C for $RuO_2$ Film with 7 Coatings

## 3.6 Effect of Firing Time on the Sheet Resistance:

Since films fired at $500^0$C and $550^0$C had the minimum sheet resistance, they were chosen for further experiments with increasing duration of firing. The value of sheet resistance for samples fired at fixed temperatures $500^0$C and $550^0$C with first layer fired for 10 minutes and the remaining for 2 minutes, 5 minutes, and 10 minutes each are tabulated in Table 3.3 and its variation with firing time is shown in Figure 3.6. Note that in figure 2 minutes, 5 minutes and 10 minutes represents the firing time of second and subsequent layers.

It is observed from Figure 3.6 that increasing the firing time from 2 minutes to 5 minutes of second and subsequent layers have no effect on sheet resistance of $RuO_2$ film while a firing time of 10 minutes increases the sheet resistance of $RuO_2$ film to higher values. This is most probable due to shrinkage of the film on firing for longer duration.

Table 3.3: Sheet Resistance of 7 Coatings $RuO_2$ Films Fired for Different Times

| Time(min.) | Sheet resistance (ohm/sq.) | |
|---|---|---|
| | $500^0$C | $550^0$C |
| 2 | 7.25 | 7.79 |
| 5 | 7.34 | 8.72 |
| 10 | 19.24 | 21.67 |

Table 3.4: Sheet Resistance with increased Film Thickness for Film Fired at $550^0$C for Different Times

| No. of Coatings | Sheet resistance (ohm/sq.) | |
|---|---|---|
| | t = 2 min. | t = 10 min. |
| 7 | 7.79 | 21.67 |
| 14 | 4.21 | 11.58 |
| 21 | 2.40 | 6.87 |

## 3.7 Effect of Film Thickness on Sheet Resistance:

In order to confirm the effect of film thickness on the sheet resistance two groups of samples were prepared. In the first group, three samples of 7 coatings, 14 coatings and 21 coatings were prepared at $550^0$C with firing time such that first layer is fired for 10 minutes, and rest of the layers for 2 minutes. In second group the firing time was chosen as 10 minutes for each layer.

The values of sheet resistance at various film thickness is tabulated in Table 3.4 and Figure 3.7 and 3.9 shows its variation with film thickness. It is observed that sheet resistance is decreasing linearly with film thickness, confirming that it it is mainly the film thickness which is controlling the sheet resistance. Since the film thickness is expected to vary approximately linearly with number of coatings, the sheet resistance is normalized to number of coatings and plotted in Figure 3.8 and 3.10. The constancy of normalized values is a clear indication that differences in sheet resistance is due to difference in thickness. This conclusion gets further support from RBS measurements as well.

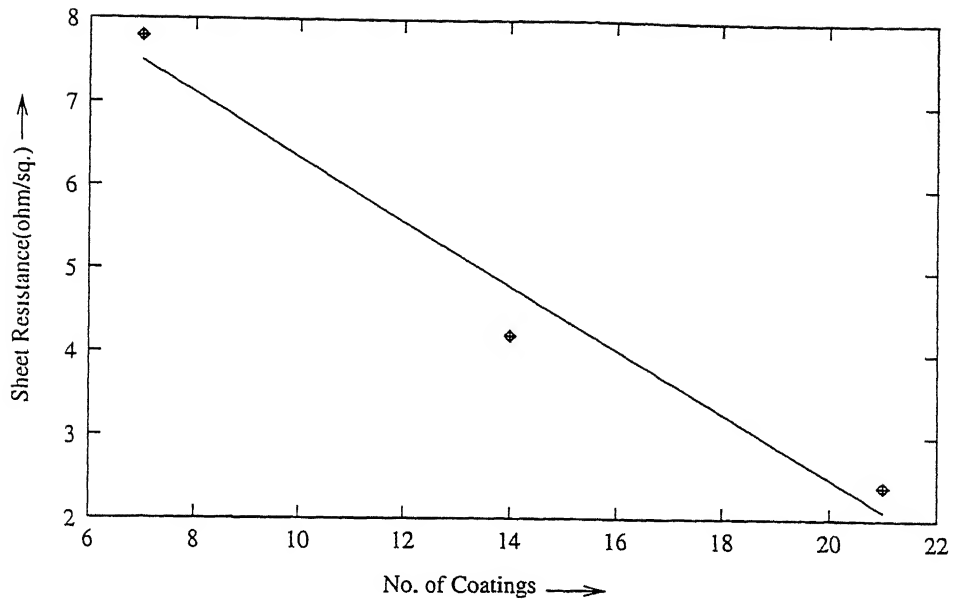


Figure 3.7: Variation of Sheet Resistance with no. of coatings(Film Thickness) at Constant Firing Time of 10 min. first layer and 2 min. rest layers at $550^0$C.

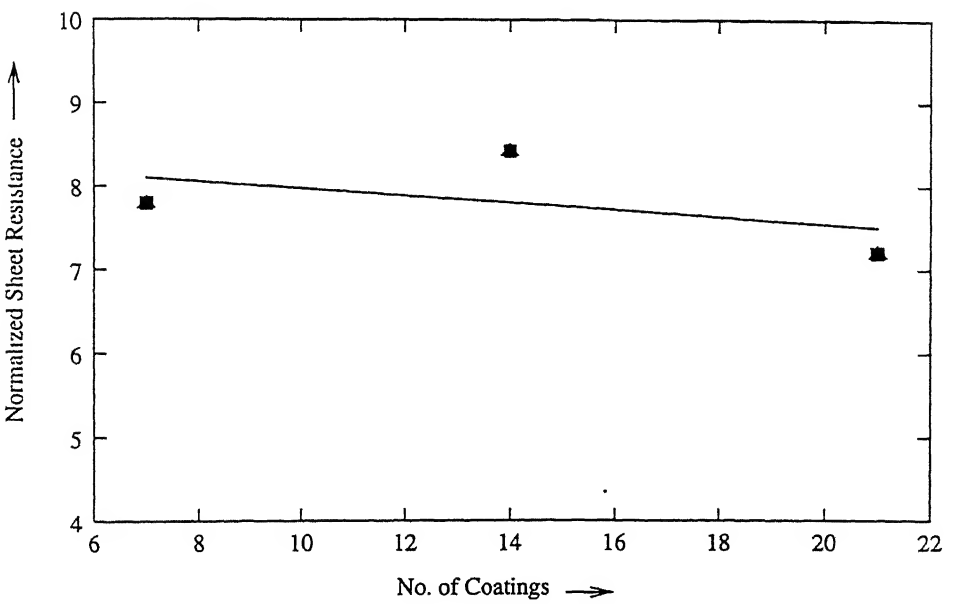


Figure 3.8: Sheet Resistance normalized to no. of Coatings at $550^0$C.for 2 min. firing

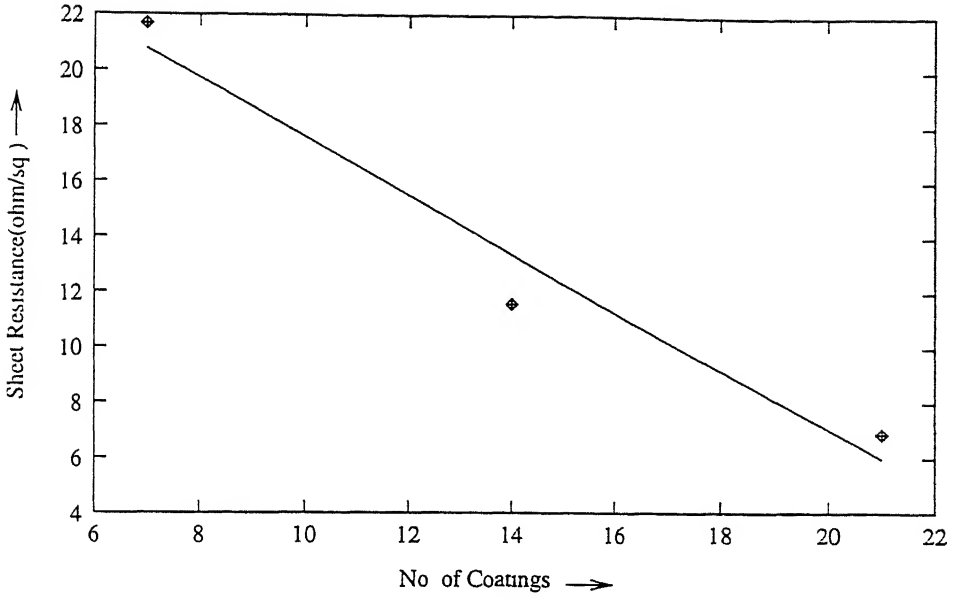


Figure 3.9: Variation of Sheet Resistance with no. of coatings(Film Thickness) at Constant Firing Time of 10 min. each layer at $550^0$C for 10 min. firing

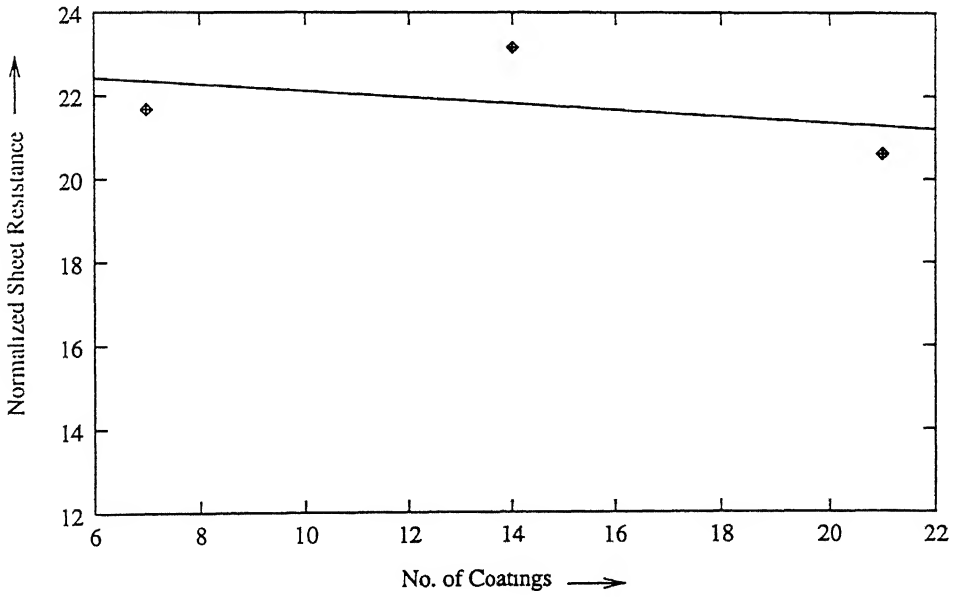


Figure 3.10: Sheet Resistance normalized to no. of Coatings at $550^0$C.

## 3.8 Rutherford Back-scattering Spectroscopy:

As it is mentioned in section 3.3.1 that increase in the sheet resistance of $RuO_2$ films heat treated at higher temperatures could be either due to intermixing of elements at $RuO_2$/Si interface and/or shrinkage in film thickness. We have used Rutherford Backscatter Spectrometry (RBS) to investigate possibilities of diffusion and change in film thickness with firing temperatures. $RuO_2$ films of seven coatings fired at various temperatures with same firing times are used for this study. Figure 3.11 shows the RBS spectra in which the surface positions of Pb, Ru, Si and Oxygen are indicated in the Figure. The spectra due to films fired at $400^0$C and $500^0$C could be simulated well using RUMP (11). For the other higher temperatures such simulations were rendered difficult due to presence of small amount of Pb, Zr, Ti and Ce in the spectra. The origin of these elements in the spectra were traced to contaminants in the furnace used for annealing. The same furnace is routinely used for heat treatment of PZT films. For temperatures higher than $500^0$C a small amount of these elements seem to that deposited on the surface of the film. since the sample is prepared through multiple coating with heat treatment for each coating, these elements appear to be uniformly distributed in the film. Therfore the uniform concentration of these trace elements should not be constrained to be due to diffusion at these temperatures.

The spectra due to low temperature fired samples ($400^0$C and $500^0$C), which could be simulated well (Figure 3.12) corresponds to simulated structures as give in Figure 3.13.The changes in the width of Ru peak clearly indicates that the film thickness changes on heat treatment. The shrinkage was approximately 100Å in going from firing temperature of $400^0$C to $500^0$C. This continues to occur for higher temperatures. The other important observation is that change Si surface position clearly indicated diffusion of Si in to the sample for heat treatments at of $500^0$C. The diffusion of Si appears to be confined to relatively small regions in the interface. Hence long duration annealing athigher temperatures is clearly to be avoided. ·If we use the thickness obtained from simulation for $500^0$C for calcualting resistivity from sheet resistance, we get a value of (1.41 $\mu\Omega$m). Earlier we shown that the decrease of sheet resistance was linear with number of coatings, and it increses due to film at temperature above $550^0$C. RBS results clearly show that film thickness is decreasing with increase in firing temperatures. Hence changes in sheet resistance in both cases can be attributed to changes in thickness

of the films. the observed resistivity of $RuO_2$ films is better than those reported by Tressler et al (7) and is comparable to best result reported for (30-100 $\mu\Omega$cm.).

It is unlikely that Si diffusion in to the film is adversely offsetting the resistivity of the films. The temperature dependence of resistivity as reported (8) shows that it is dominated by phonons at temperatures above 100 K. Si as an impurity would only change restivity due to impurity scattering at low tempeature (below about 100 K). Hence $RuO_2$ films can indeed be used for metallic contacts inspite of some amount of diffusion of silicon. However, as has been shown by others it does provide a good barrier for diffusion to Pb in PZT processing.

## 3.9 Growth of Sol-gel Derived PZT Thin Film on $RuO_2$ Coated Si Substrate:

As has been pointed out in chapter 1 the motivation for developing good quality $RuO_2$ films has been to use them as electrode and a barrier layer in PZT devices. In this section we present results on growth of sol-gel derived PZT thin films on $RuO_2$ films coated on silicon.

## 3.10 Sample details:

The $Pb_1.05(Zr_0.53\ Ti_0.47)O_3$ thin films used in this work are prepared by sol-gel method. The phase formation behaviour of PZT thin films has been studied on $RuO_2$ coated Si substrate. We have selected 21 coatings of $RuO_2$ thin film fired at $550^0$C with first layer fired for 10 minutes and subsequent layers for 2 minutes each. From previous work (Subhasis thesis) it is estimated that such a PZT film used have a thickness of 0.5 $\mu$m.

During repeated coating of PZT films the film is fired at $400^0$C in air for 10 minutes after each coating. After obtaining the desired thickness the film is annealed at $700^0$C for 2 minutes in air or in $O_2$ ambient.

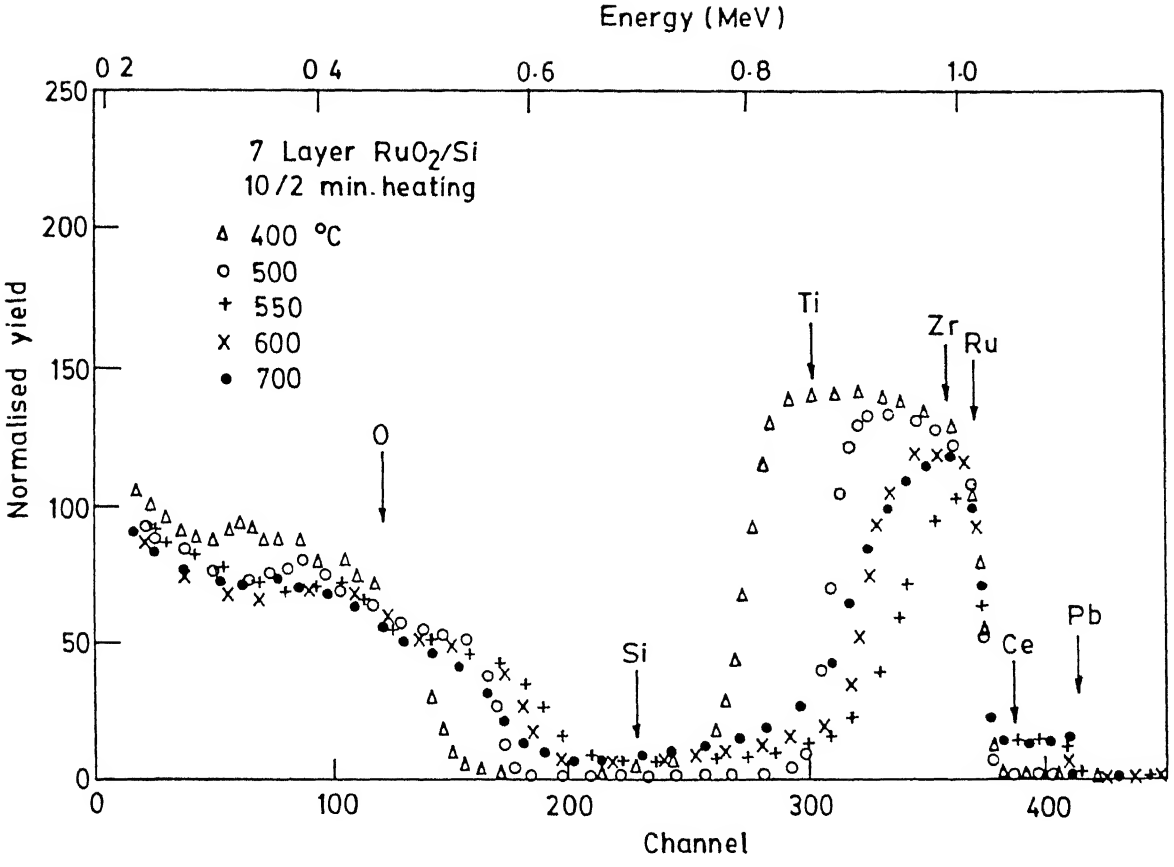


Figure 3.11. RBS Spectra of Seven Layered $RuO_2$ Films Fired at Various Temperatures with First Layer Fired for 10 min and Subsequent Layers for 2 min.

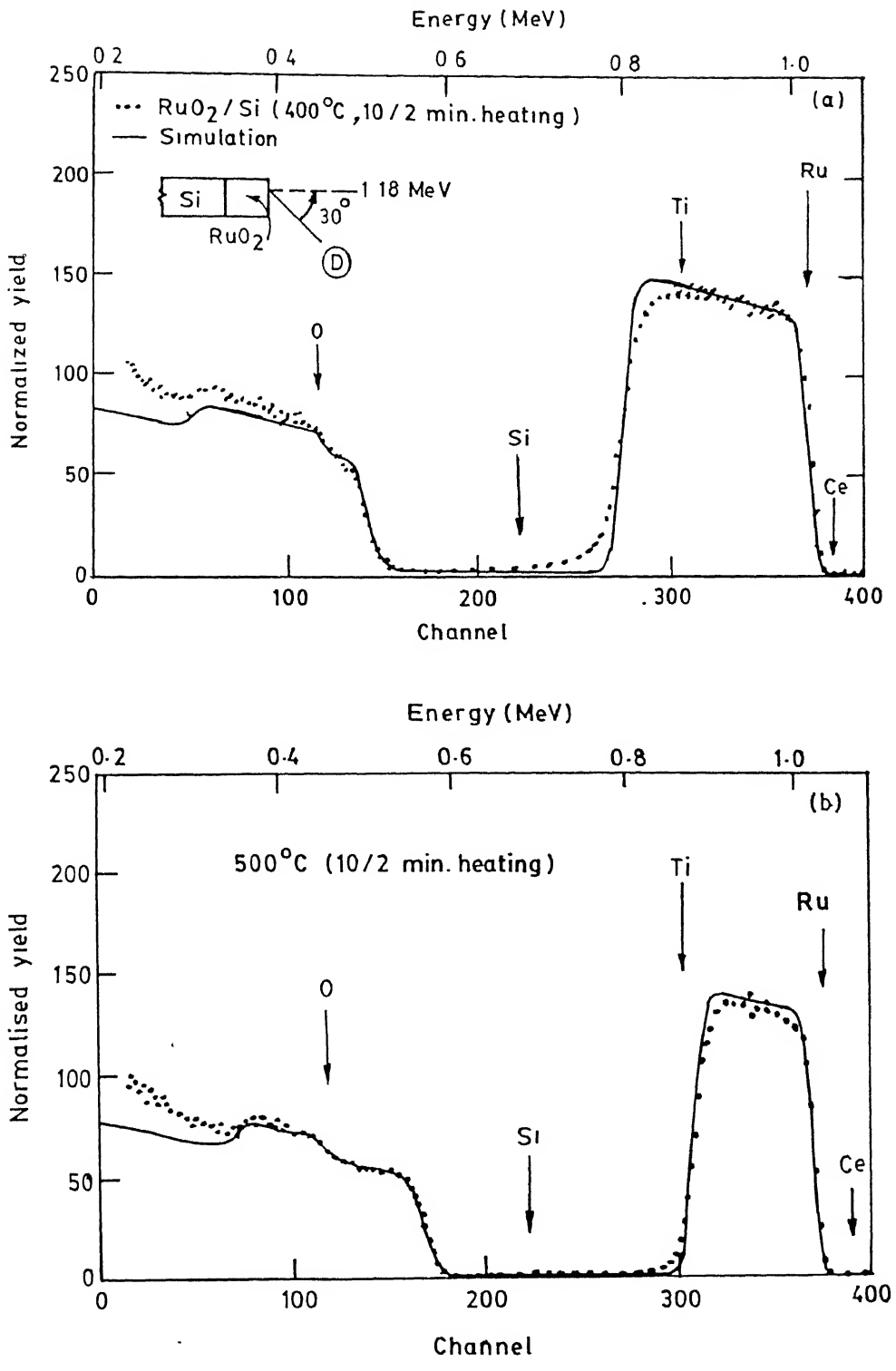


Figure 3.12: Simulated RBS Spectra of Seven Layered RuO−2 Films Fired at (a) $400^0$ (b) $500^0$C,arrows indicate surface positions of element shown.

| Firing Temperature ($^{o}$C) | RBS Simulation Structure | Layer thickness (Å) | Layer No. |
|---|---|---|---|
| 400 | $RuO_2$ $Pb_{0.002}$ | 1950 | 1 |
| | $SiO_2$ | 200 | 2 |
| | $Ru_{0.003}$ Si | 10000 | |
| 500 | $RuO_2$ $Pb_{0.002}$ | 3000 | 1 |
| | $Ru_{0.003}$ Si | 10000 | |

Figure 3.13: Summary of RBS Results for Seven Layered $RuO_2$ Fims on Silicon Fired at (a) $400^0$ (b) $500^0$C.

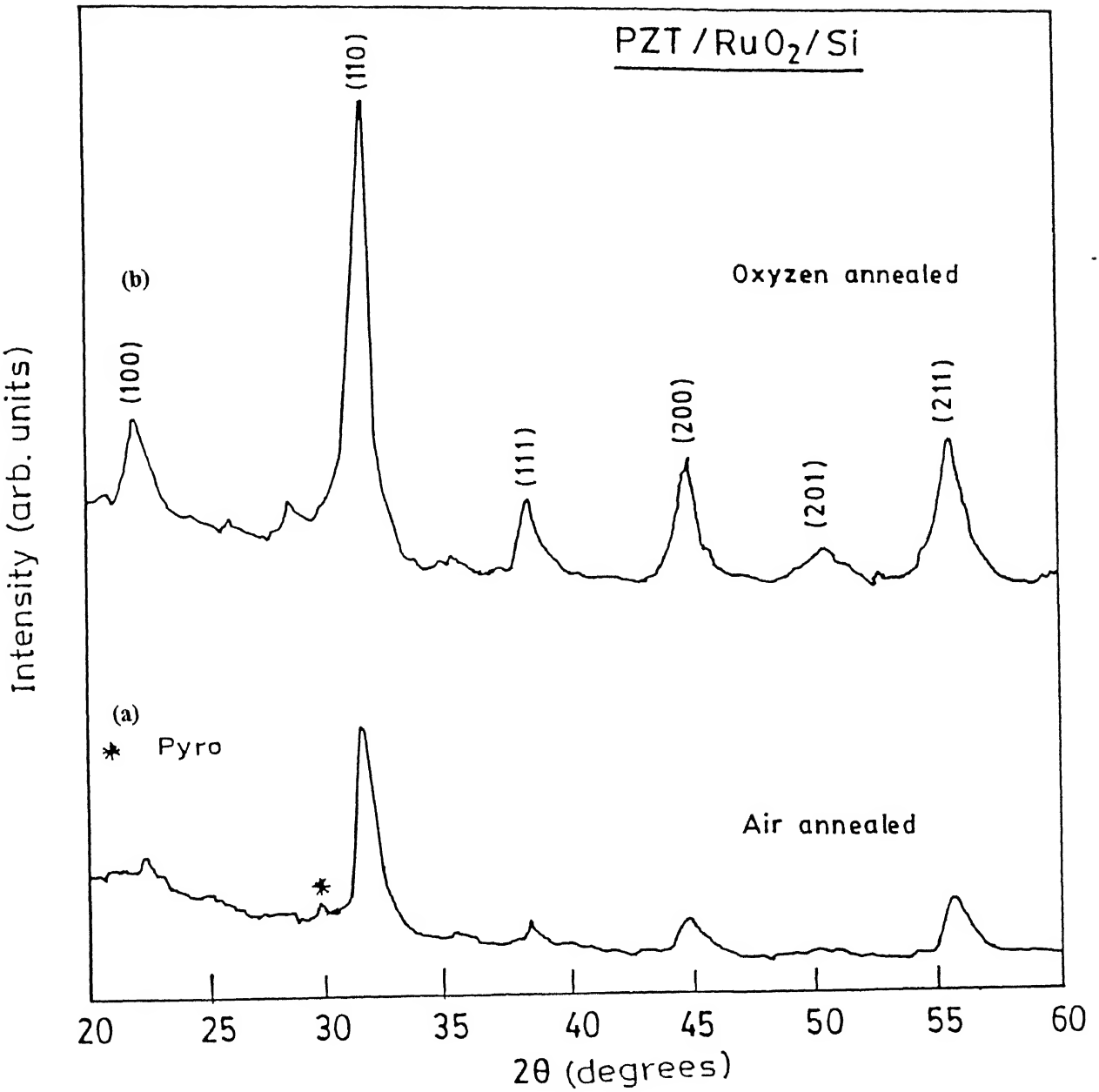


Figure 3.14: X-Ray Diffractograms from PZT Films (a) air annealed (b) oxygen annealed on $RuO_2$ Coated Si

## 3.11 Phase formation behaviour:

In this section we have presented the phase formation behaviour of PZT thin film on $RuO_2$ coated Si. Figures 3.14 shows the X-ray diffraction patterns of PZT thin films of thickness 0.5 $\mu$m fired at $400^0$C and annealed at $700^0$C in air or in oxygen. The peaks have been indexed according to JCPDS diffraction file (14) and data is reproduced in Table 3.5 In case of air annealing the PZT film (25 mole% excess PbO) crystallises into perovskite phase a small amount of pyrochlore phase. The small peak at $2\theta = 30^0$ indicates the presence of small amount of pyrochlore phase. For the film annealed in $O_2$ the peaks are sharper and the peak due to pyrochlore is of much less intensity.

From the above results it is clear that perovskite phase in PZT films easily form on $RuO_2$ coated Si substrates. It is also observed that oxygen annealing helps to obtain better crystallinity of perovskite phase as compared to air annealing.

The above results of pervoskite phase formation of PZT thin film on $RuO_2$/Si system are in agreement with the fact that $RuO_2$ acts as a diffusion barrier to Pb On a bare Si substrate the PZT film forms in pyrochlore phase no perovskite phase is obtained. It has been shown (2) that this is principally due to large amount of Pb diffusion from PZT film in to Si substrate. Thus the $RuO_2$ film prepared from the solution chemistry technique is quite effective as a diffusion barrier for Pb in to Si.

## 3.12 Microstructural Study of PZT Thin Film on $RuO_2$ Coated Si:

The micro structure of perovskite phase usually consists of very fine crystallites within grain like features. The results of our experiments on high temperture iso thermal annealing of PZT films are as follows. Figure 3.15 show the microstructures of 0.5 $\mu$m thick $Pb_1.05ZT$ films on $RuO_2$/Si system heat treated at $700^0$C for 2 minutes in air and in oxygen ambient respectively. As already mentioned while presenting the phase analyses, the $700^0$C/2 minutes treatment in air results in mostly a perovskite phase. The micro structure shows combination of a large numbers of small grains along with relatively larger grains of several micron diameter. Similar results have also been reported by Majumder et al (3) for PZT films on Pt substrate but with higher annealing time eg. one hour at $700^0$C.

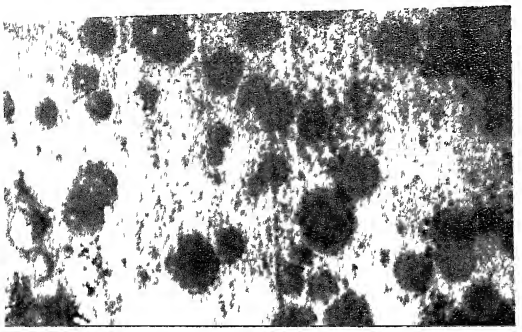


(a)


(b)

Figure 3.15: Micro-structures of PZT Films (a) air annealed (b) oxygen annealed on $RuO_2$ Coated Si

The micro structure of PZT film treated at $700^0$C/2 minutes in oxygen consists of nearly uniform grain with well developed grain boundaries.The degree of crystallization of films in this case appears to be better than that of air annealed film. The growth of perovskite crystallites is favoured in $O_2$ ambient. So that better crystallinity appears in this case. This is also indicated X-ray results presented in the previous section.

In the light of micro-structures presented above it can be concluded that in case of air annealing of PZT film on $RuO_2$/Si system at $700^0$C for 2 minutes, first larger grains developed which breaks in to finer grains and coalesce to form grain like clustures. In any case, from processing point of view, annealing in oxygen ambient seems to accelerate crystallization process resulting in well developed crystallization even for such a small annealing time.Thus it can be concluded that annealing in oxygen favours the perovskite phase formation in case of PZT film grown on $RuO_2$ coated Si.

Electrical characterization, specially P-E hysteresis loop measurements require PZT film thickness to be more than approximately 0 6$\mu$ This would need about 14 spin coated layers to achive the desired thickness . During the course of this work, this was attempted several times. However it was found that PZT films peel off after about 12 coatings. This is most probably due to stresses that developed in the film as thickness increased. There are several reports (15) in which the stress in film due to electrode has been identified as a cause of peeling off of films. In our work we observe the occurence of a well defined critical thickness for this to occur.

Further electrical characterization of films prepared by the present process would be possible by finding a way of avoiding tensile stresses in the film.

# Chapter 4

# Conclusions

Thin films of lead zirconate titanate (PZT) have many applications including that of nonvolatile random access memory in computer systems. For commercial applications of ferroelectric devices there is need of making these devices on Silicon. In coupling ferroelectric processing with Silicon technology, one of the mejor prblems is the diffusion of Pb from PZT film into Silicon substrate. The difficiency of Pb in PZT film results in pyrochlore phase formation while for device applications perovkiste phase needed. This diffusion of Pb in to the substrate can be prevented by interposing a suitable barrier layer. This barrier layer must be conducting to avoid the use of any additional conducting layer for bottem electrode. Further, occurence of fatigue, ie. the reduction in remenent polarization with repeated switchings, is a limiting factor for the performence of ferroelectric devices. The entrapment of oxygen vaccancies at the interface of electrode and ferroelectric film is mainly responcible for this. It is believed that oxide electrode can provide better fatigue resistance by reducing oxygen vacancy pile up at the interface by exchanging oxygen vacancies with the oxygen in oxide electrode. Ruthenium Oxide ($RuO_2$) is one of the conducting ceramic oxides having metal-like conductivewith excellent diffusion barrier property and thermal stability at elevated temperatures. This work is devoted to the growth and study of $RuO_2$ films for a variable conducting oxide applications. In this work our primary goals have been,

- Optimization of processing parameters of $RuO_2$ thin films grown by solution chemistry technique on Si substrate to achieve high quality $RuO_2$ films with good conductivity.

- Evaluation of suitability of $RuO_2$ coated Si substrates for growth of perovskite phase PZT films by sol-gel method.

Crackfree $RuO_2$ thin films have been prepared on Si substrates by solution- chemistry technique. In order to study the effect of processing parameters on the conductivity of $RuO_2$ film two different set of heat treatments, (Isothermal and Isochronal) have been used. In case of isochronal heat treatment the firing temperature were varied keeping firing time constant, and in isothermal heat treatment duration of firing were varied at fixed firing temperatures. The effect of film thickness on conductivity has also been studied. The PZT films were grown on RuO−2 coated Si substrate by sol-gel method. air and oxygen annealing of PZT films were done to study the crysttalization of PZT film.

Routine characterization of samples has been carried out using several techniques including X-ray diffraction for phase analysis, SEM for microstructural study, Resisty measurement and RBS for studying diffusion profile. Some of the significant observations and conclusions of this work are listed below:

- Good quality $RuO_2$ films have been successfully grown on Si substrates using solution chemistry technique.

- The XRD peaks indicate that crystallization of $RuO_2$ is completed at about $500^0$C. Little broadning of XRD peaks above $550^0$C indicate small amount of intermixing of elements at $RuO_2$/Si interface at higher temperatures.

- Microstructures of films indicate that grain size and surface roughness of the films increases for higher firing temperatures (eg. 600 and $700^0$C) and higher firing times (eg. 10 minutes firing) of each layer. Firing the film for 10 minutes results in crater like film surface.

- Sheet resistance of $RuO_2$ is found to be minimum for treatment at $500^0$ and $550^0$C, however sheet resistance increases for firing at temperatures of $600^0$ and $700^0$C for fixed firing time.

- Sheet resistance of $RuO_2$ is constant for firing times of 2 minutes and 5 minutes of subsequent layers whereas it inreases to higher value on firing each layer for 10 minutes.

- . Sheet resistance of $RuO_2$ film is found to decrease with film thickness, however sheet resistance normalized with film thicness shows constancy which indicates that the changes in sheet resistance can be attributed to change in film thickness.

- RBS spectra of samples fired at various clearly shows decrease in film thickness with increased firing temperature at fixed firing times. Small amount of diffusion of silicon in the $RuO_2$ film is also observed at higher temperatures. This signifies that firing at $550^0$C is optimum for such application.

- Crack free PZT films are successfully grown on Si substrates coated with $RuO_2$ by sol-gel method.

- Pervoskite phase was obtained in all the PZT films. Films annealed in $O_2$ ambient show only perovskite, while those annealed in air also contains small amount of pyrochlore phase. XRD peaks in case of $O_2$ annealed films are more intense and sharper than that of air annealed films indicating that crystallization of PZT film is favoured in $O_2$ ambient.

- On the basis of micro-structural study it is concluded that in case of air annealing, initially larger grains appear which breaks into fine grains and then coalesce to form grain like clustures. However in case of $O_2$ annealing this process is found to be accelerated, and well developed crystallization results even for short duration annealing of 2 minutes.

In summary, we have prepared smooth, fine grained $RuO_2$ thin films with good conductivity on silicon substrates using solution chemistry techniques. We have shown that short firing times (eg. 2 to 10 minutes) at temperatures between 500 - $550^0$C results in the $RuO_2$ films with enough conductivity which is perfectly acceptable forunder layer electrode application for PZT thin film devices. Finally, $RuO_2$ coated Si substrates have been successfully used to grow PZT films which crystallises in the desired perovskite phase.

## 4.1 Scope for Future Work:

During the course of this work it was found that on increasing the thickness of PZT layers on $RuO_2$ films beyond a critical value, the PZT layer peel off most probably due to prescence of tensile stresses. Detailed electrical characterization of PZT films require thickness to be greater than 0.6 $\mu$m.

Hence, further electrical characterization of the films prepared by the present process would be possible by finding a way of avoiding such tensile stresses in the film.

# Bibliography


[1] B. Jaffe, W.R. Cook and M. Jaffe, Piezoelectric Ceramics, Academic Press, London (1971).

[2] S B. Desu and I.K. Yoo, Proc. Inter. Symp. Appl. Ferroelectrics ( ISAF-92), M. Liu, A Safari, A. Kingo and G. Hartline (Eds) IEEE Proc.(1992) pp 412.

[3] S.B. Majumder, D.C. Agrawal, Y.N. Mohapatra and V.N. Kulkarni, *Integrated Ferroelectrics* 9 pp 271-284 (1995).

[4] S.B. Krupanidhi, H. Hu and V Kumar,*J. Appl. Phys.*, 71 376 (1992)

[5] N.R. Parikh et al.,*Mat. Res. Sympo. Proc.* 200, 193 (1990)

[6] D P. Vijay and S.B. Desu, *J. Electrochem. Soc.*, Vol.140 , No. 9, Sept 1993.

[7] J.F. Tressler, K. Watanabe, M. Tanaka, *J. Am. Ceram. Soc.*, 79 [2] 525-29 1996.

[8] L. Krusin-Elbaum, M. Wittmer and D.S. Yee, *Appl. Phys. Lett.*, Vol. 50, No. 26, 29 June 1987.

[9] J.J. Lee, C.L. Thio, and S.B. Desu, *J. Appl. Phys.*, 78, 5073 (1995).

[10] G. Yi and M. Sayer, *Cerm. Bull.*, 70, 1173 (1991).

[11] L.R. Doolittle, *Nucl. Inst. Method*, 15, 227 (1986).

[12] Philips Res. Rep., B, 13 (1958) 1.

[13] Y. Murakami, S. Tsuchiya, K. Yahikozawa, and Y. Takasu, *J. Mater. Sci. Lett.*, 13, 1773-74 (1994).

[14] JCPDS File (1996).